Thesis

On

EXPERIMENTAL STUDY ON FIBER LASER BEAM MACHINING

Submitted in partial fulfillment of the requirement for the award of degree of

MASTER OF ENGINEERING
IN
PRODUCTION & INDUSTRIAL ENGINEERING

Submitted By

Akashdeep Singh
Roll No. 801182001

Under the guidance of

Dr. Vinod Kumar Singla
Associate Professor
Thapar University,Patiala

DEPARTMENT OF MECHANICAL ENGINEERING
THAPAR UNIVERSITY
PATIALA-147004, INDIA

JULY, 2013

DECLARATION

I hereby declare that the thesis entitled '**Experimental Study on Fiber Laser beam machining**' is an authentic record of my study carried out as requirement for the award of degree of **Master of Engineering** in **Production and Industrial Engineering** at **Thapar University, Patiala** under the supervision of **Dr. Vinod Kumar Singla**, Associate Professor, Thapar University, Patiala during July 2012 to July 2013. The matter embodied in this report has not been submitted in part or full to any other university or institute for award of any degree.

Date: 15/07/2013

Akashdeep Singh

It is certified that the above statement made by the student is correct to best of my knowledge and belief.

(Dr. Vinod Kumar Singla)
Associate Professor
Mechanical Engineering Department
Thapar University,Patiala-147004

Countersigned By

(Dr. AJAY BATISH)
Professor and Head
Mechanical Engineering Department
Thapar University, Patiala-147004

(Dr. S. K. MOHAPATRA)
Dean of Academic Affairs
Thapar University, Patiala-147004

ACKNOWLEDGEMENT

With deep sense of gratitude I express my sincere thanks to my guide **Dr. Vinod Kumar Singla**, Associate Professor, Mechanical Engineering Department, Thapar University, for his valuable guidance, proper advice and constant encouragement during this thesis work. I found his guidance to be extremely valuable. I also feel very much obliged to **Dr. Ajay Batish**, Professor and Head, of Mechanical Engineering Department.

I would also like to thank all the members and employees of Mechanical Engineering Department, Thapar University, Patiala for their everlasting support.

I am also thankful to my friends for their cooperation. I would like to extend my gratitude to all those persons who directly or indirectly helped me in process and completion of this work.

Akashdeep Singh

ABSTRACT

Laser Beam Cutting (LBC) is one of the most widely used manufacturing techniques for generation of accurate and complex geometrical shapes on ferrous metal, non ferrous metal, stones, plastic and ceramics components with high dimensional accuracy. Fiber lasers are solid state laser technologies that offer a combination of high beam quality and a wavelength that is easily absorbed by metal surfaces. This work aims to evaluate the optimum laser cutting parameters for 0.5 mm thickness of mild steel sheets by using Fiber laser beam machine of 100 W power and oxygen as assist gas. Focus of work is mainly on output response parameters like Material Removal Rate (MRR), Kerf Width (K_W) and Kerf Deviation (K_D). Results are analysed using Analysis of Variance (ANOVA) technique. The effect of different input process parameters like feed rate, laser power, frequency and gas pressure is studied on the output responses.

ABBREVIATIONS

ANOVA	Analysis of Variance
MRR	Material Removal Rate
K_W	Kerf Width
K_D	Kerf Deviation
LBM	Laser Beam Machine
LBC	Laser Beam Cutting
OA	Orthogonal Array
DOF	Degree of freedom
S/N ratio	Signal to noise ratio

CONTENTS

LIST OF FIGURES

LIST OF TABLES

CHAPTER 1

INTRODUCTION

1.1 INTRODUCTION TO NON TRADITIONAL PROCESSES

Advanced industries like automobiles, turbines, missiles, nuclear reactors, etc. requires materials like high strength temperature resistant alloys which have high strength, toughness, corrosion resistance and other various properties. With rapid development in the field of materials, it has become essential to develop cutting tool materials and processes which can safely and conveniently machine such new materials for productivity, high accuracy. Consequentially, nontraditional techniques of machining are providing effective solution to the problems imposed by increasing demand for high strength temperature resistant alloys, which otherwise was very difficult to machine with conventional methods. The processes are non conventional in the sense that they do not use conventional tool for machining purpose. Instead these utilize energy indirectly to remove material from work piece. These techniques can be classified into three categories, i.e. mechanical, electro thermal and electro chemical machining processes. The mechanical non- conventional techniques (Abrasive Jet Machining, Ultrasonic Machining, Water Jet Machining, Abrasive Water Jet Machining) utilizes energy of either abrasive particles or a water jet to remove the material. In electro thermal processes (laser beam machining/cutting, electron beam machining) the energy is supplied in the form of heat, light, and electron bombardment which results melting or vaporization and melting both of work materials and in electro chemical machining, an anodic dissolution process is carried on to remove material. The selection of process depends on various factors like physical parameters, shape to be machined, properties of work piece material to be cut and economics of the process.

1.2 LASER BEAM MACHINE (LBM)

Laser is an acronym for light amplification by stimulated emission of radiation. It is essentially a coherent, convergent and monochromatic beam of electromagnetic radiation with wavelength ranging from ultraviolet to infrared. Emergence of advanced engineering materials, stringent design requirements, intricate shape and unusual size of work piece restrict the use of conventional machining methods. Hence, it was realized to develop some nonconventional machining methods known as advanced machining processes. LBM is one of the advanced machining processes which are used for shaping almost whole range of engineering materials. The laser beams are widely used for cutting, drilling, marking, welding, sintering and heat treatment. The laser is also used to perform turning as well as milling operations but major application of laser beam is mainly in cutting of metallic and non-metallic sheets.

1.3 HISTORY ABOUT LASER BEAM

Planck has given the concept of quanta in 1900 and in 1920 it was well accepted that apart from wavelike characteristics of light it also shows particle nature while interacting with matters and exchange energy in the form of photons. The initial foundation of laser theory was laid by Einstein who has given the concept of stimulated emission in 1917, though the first industrial laser for experimentation was developed around 1960s. Townes and Shawlow (1957) produced the first laser known as Ruby Laser (Dubey 2007).

1.4 LASER BEAM CUTTING-THE LASING PROCESS

Lasing process describes the basic operation of laser, i.e. generation of coherent (both temporal and spatial) beams of light by light amplification using stimulated emission. The three processes required to produce the high energy laser beam are, stimulated emission, population inversion and amplification.

1.4.1 SPONTANEOUS EMISSION

In the model of atom, negatively charged electrons rotate around the positively charged nucleus in some specified orbital paths. The geometry and radii of such orbital paths depend on a variety of parameters like number of electrons, presence of neighboring atoms and their electron structure, presence of electromagnetic field etc. Each of the orbital electrons is associated with unique energy levels. At absolute zero temperature an atom is considered to be at ground level, when all the electrons occupy their respective lowest potential energy. The electrons at ground

state can be excited to higher state of energy by absorbing energy form external sources like increase in electronic vibration at elevated temperature, through chemical reaction as well as via absorbing energy of the photon. Fig. 1.1 depicts schematically the absorption of a photon by an electron. The electron moves from a lower energy level to a higher energy level. On reaching the higher energy level, the electron reaches an unstable energy band. And it comes back to its ground state within a very small time by releasing a photon. This is called spontaneous emission. Schematically the same is shown in Fig. 1.1 .The spontaneously emitted photon would have the same frequency as that of the "exciting" photon.

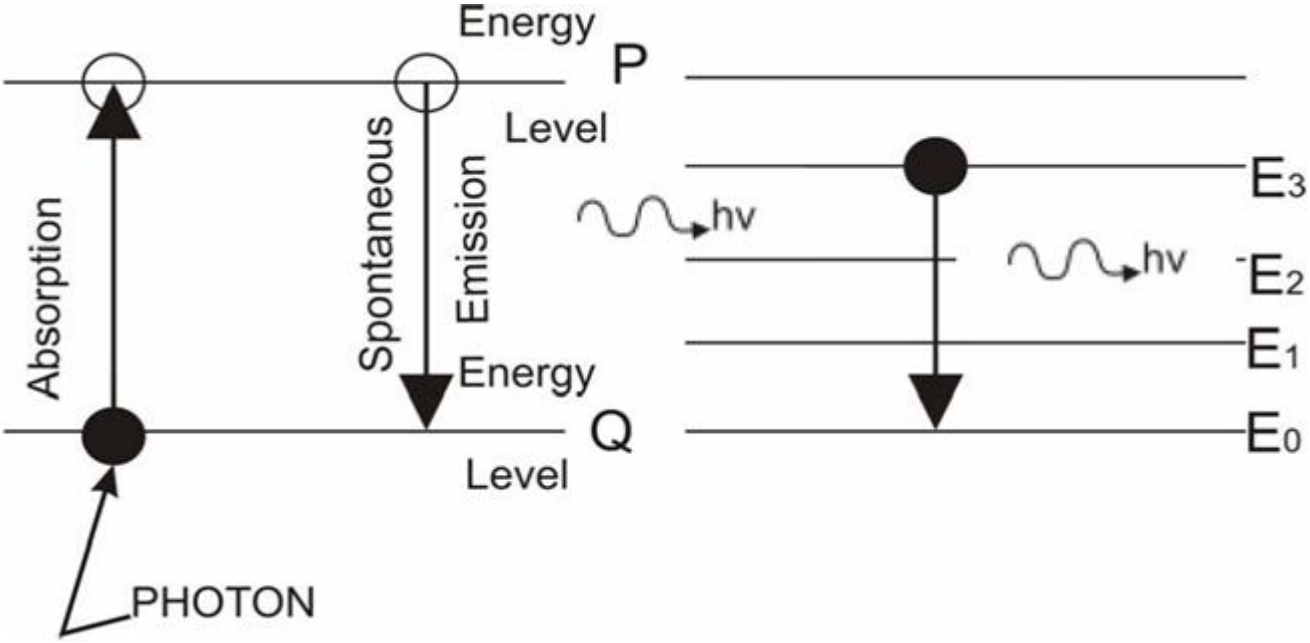

Fig. 1.1 Energy bands in materials

(http://nptel.iitm.ac.in/courses/Webcourse-contents/IIT%20Kharagpur/Manuf%20Proc%20II/pdf/LM-40.pdf)

1.4.2 STIMULATED EMISSION

Sometimes change of energy state puts the electrons in a meta-stable energy band. Instead of coming back to its ground state immediately, it stays at the elevated energy state for micro to milliseconds. In a material, if more number of electrons can be somehow pumped to the higher meta-stable energy state as compared to number of atoms at ground state, and then it is called population inversion. Such electrons, at higher energy meta-stable state, can return to the ground state in the form of an avalanche provided stimulated by a photon of suitable frequency

or energy. This is called stimulated emission shown in Fig.1.2. If it is stimulated by a photon of suitable energy then the electron will come down to the lower energy state and in turn one original photon, another emitted photon by stimulation having some temporal and spatial phase would be available. In this way coherent laser beam can be produced.

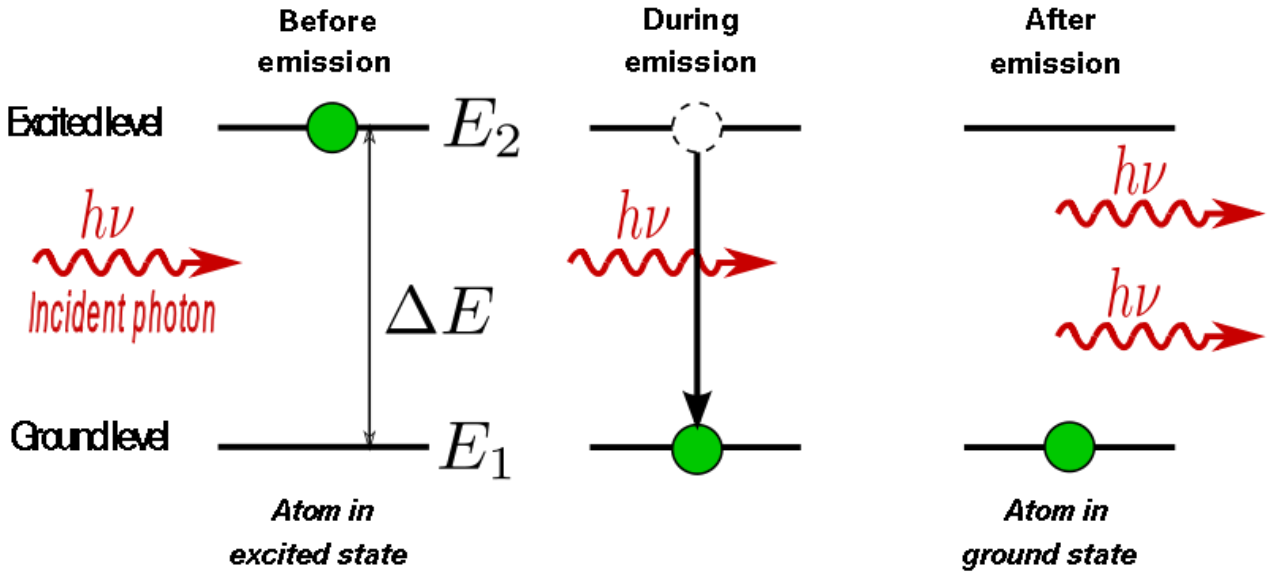

Fig. 1.2 Stimulated emissions

(http://en.wikipedia.org/wiki/File:Stimulated_Emission.svg).

1.4.3 POPULATION INVERSION

Population inversion is necessary condition for stimulated emission. Without population inversion, there will be net absorption of emission instead of stimulated emission .For a material in thermal equilibrium, the distribution of electrons in various energy states is given by the Boltzmann distribution law.

$$N_2 = N_1 \exp\left[-\left(E_2 - E_1\right)/kT\right]$$

Equation No. …….1.1

Where N1 and N2 are electron densities in state 1 and 2 with energies E1 and E2 respectively. T and K are the absolute temperature and Boltzmann constant, respectively.

According to Boltzmann's law, the higher energy states are the least populated and the population of electrons in the higher energy states decreases exponentially with energy. Population inversion corresponds to a non equilibrium distribution of electrons such that the higher energy states have a larger number of electrons than the lower energy states. The process of achieving the population inversion by exciting the electrons to the higher energy states is referred to as pumping (Svelto and Hanna 1989) .The population inversion explained here for the two level energy systems. Population inversion in the most of the lasers generally involves three or four level energy levels Fig.1.3.For a three level energy system, electrons are first pumped from energy level E0 to E2 by the absorption of radiations(of frequency =E2-E0/h)from a pumping source. The lifetime of the electrons in the higher energy level is generally very short and the electrons from the energy level E2 rapidly decay into metastable state level E1 without any radiation (radiation less decay).Thus the net population inversion is achieved between energy levels E1 and E0, which is responsible for the subsequent emission of laser radiation (Fig 1.3 a). Similar mechanisms cause the population inversion between the energy levels E2 and E1 in four level energy level systems(Fig.1.3 b)(Ready 1997).

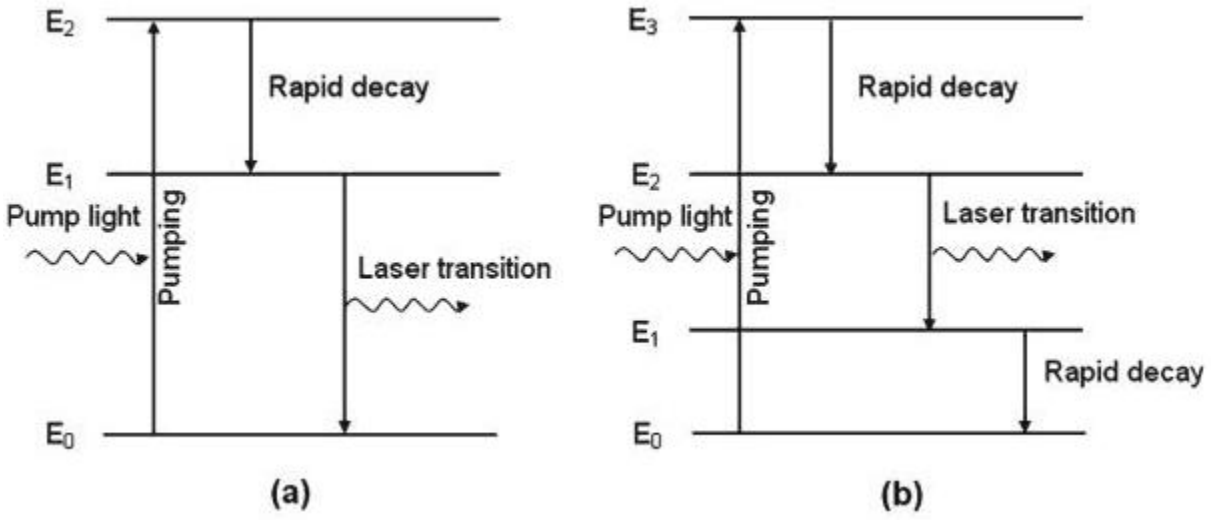

Fig 1.3 Schematic of the population inversion in (a) Three level and (b) Four level energy laser systems (dahotre, 2008).

Fig. 1.4 schematically shows working of a laser. There is a gas in a cylindrical glass vessel. This gas is called the lasing medium. One end of the glass is blocked with a 100% reflective mirror

and the other end is having a partially reflective mirror. Population inversion can be carried out by exciting the gas atoms or molecules by pumping it with flash lamps. Then stimulated emission would initiate lasing action. Stimulated emission of photons could be in all directions. Most of the stimulated photons, not along the longitudinal direction would be lost and generate waste heat. The photons in the longitudinal direction would form coherent, highly directional, intense laser beam.

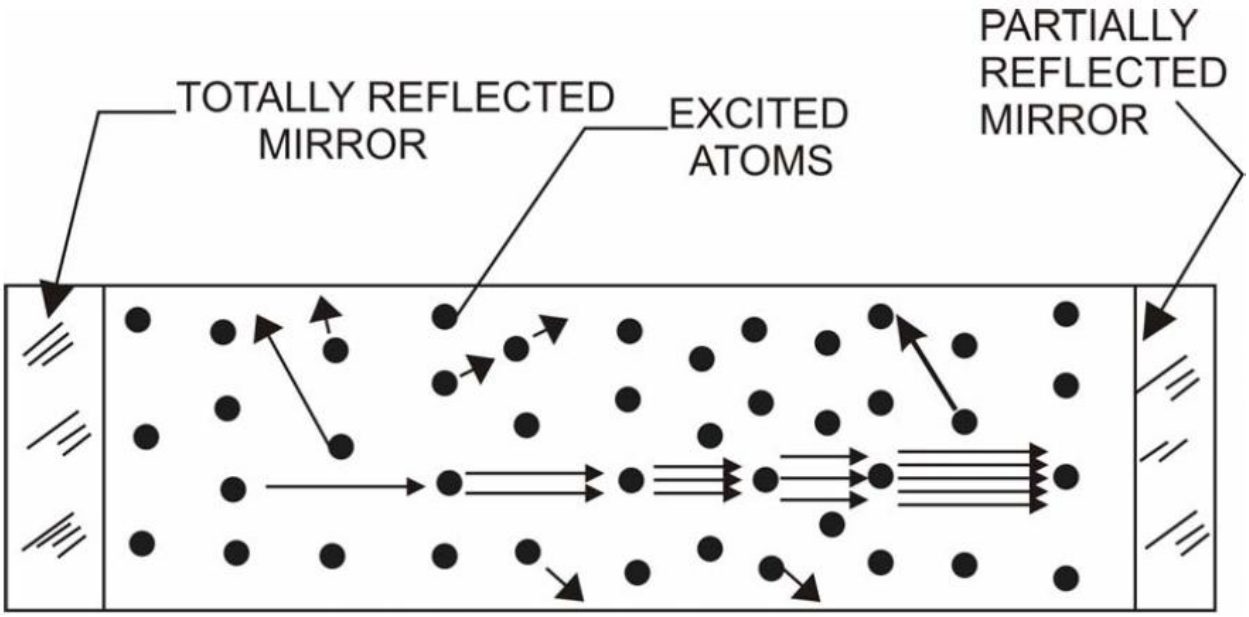

Fig. 1.4 Lasing action (http://nptel.iitm.ac.in/courses/Webcourse-contents/IIT%20Kharagpur/Manuf%20Proc%20II/pdf/LM-40.pdf)

1.5 CUTTING PRINCIPLE

The basic principle of laser beam cutting is shown in figure 1.5 .An optical lens placed in the path of laser beam is used to focus the beam and to create a focal length suitable for the specific cutting application. The distance between the lens and material is adjusted so that the focal point of the laser beam is concentrated on or below the surface of the material depending on the material process required. Material around the focal point of the beam will melt and is blown away by the assist cutting gas that is concentric to the laser beam.

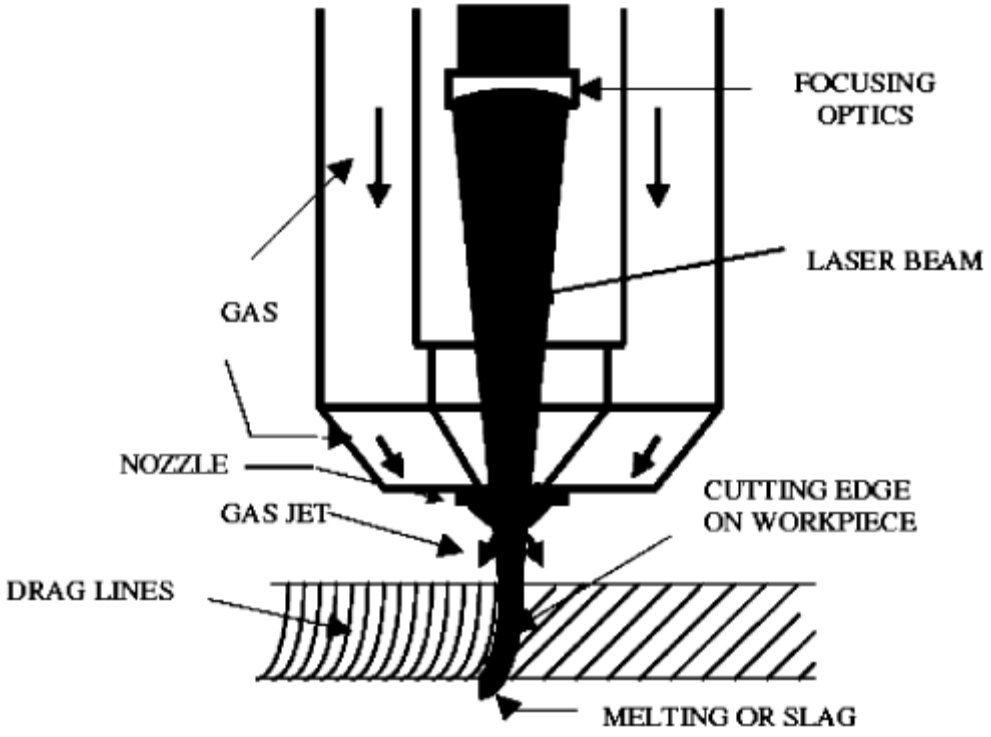

Fig. 1.5 Cutting principle (Dubey, 2008)

The mechanism of material removal during LBM includes different stages such as (i) melting, (ii) vaporization, and (iii) chemical degradation (chemical bonds are broken which causes the materials to degrade). When a high energy density laser bream is focused on work surface the thermal energy is absorbed which heats and transforms the work volume into a molten, vaporized or chemically changed state that can easily be removed by flow of high pressure assist gas jet, which accelerates the transformed material and ejects it from machining zone (Dubey and yadava 2008).

Laser beam cutting (LBC) is a thermal process. The effectiveness of this process depends on thermal properties and, to a certain extent, the optical properties rather than the mechanical properties of the material to be machined. Therefore, materials that exhibit a high degree of brittleness, or hardness, and have favorable thermal properties, such as low thermal diffusivity and conductivity, are particularly well suited for laser machining. Since energy transfer between the laser and the material occurs through irradiation, no cutting forces are generated by the laser, leading to the absence of mechanically induced material damage, tool

wear and machine vibration. Moreover, the material removal rate (MRR) for laser cutting is not limited by constraints such as maximum tool force, built up edge formation or tool chatter.

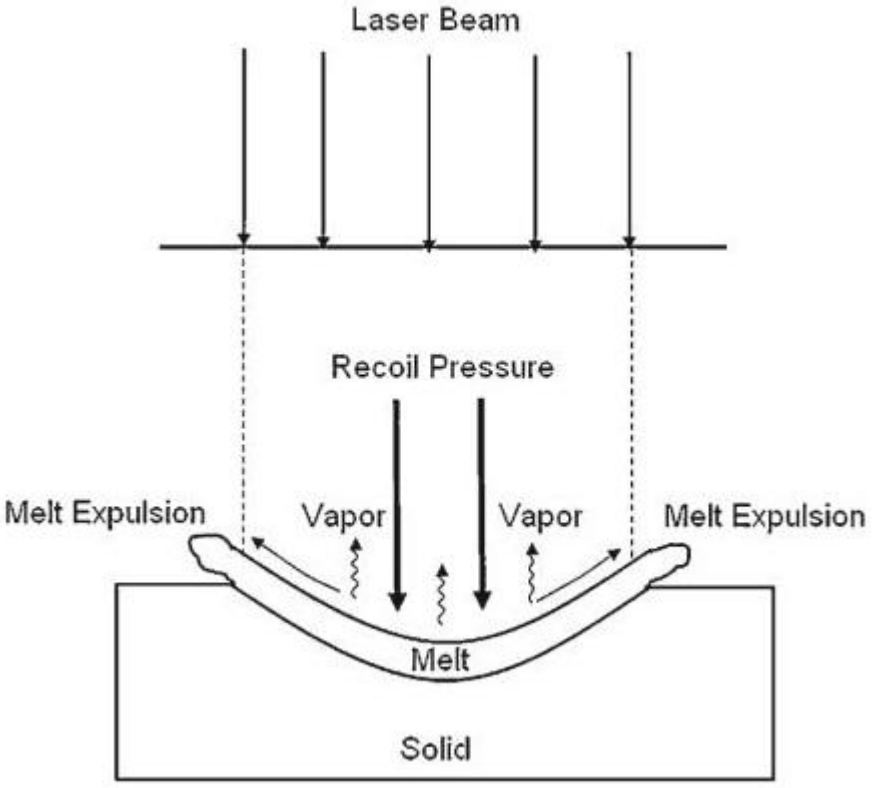

Fig. 1.6 Schematic of surface evaporation and melt expulsion processes of material removal during laser material interactions (Dahotre, 2008).

1.6 MODE OF OPERATION

A laser can be classified as operating in either continuous or pulsed mode, depending on whether the power output is essentially continuous over time or whether its output takes the form of pulses of light on one or another time scale. Of course even a laser whose output is normally continuous can be intentionally turned on and off at some rate in order to create pulses of light. When the modulation rate is on time scales much slower than the cavity lifetime and the time period over which energy can be stored in the lasing medium or pumping mechanism, then it is still classified as a "modulated" or "pulsed" continuous wave laser.

1.6.1 CONTINUOUS WAVE OPERATION

Some applications of lasers depend on a beam whose output power is constant over time. Such a laser is known as continuous wave (CW). Many types of lasers can be made to operate in continuous wave mode to satisfy such an application. Many of these lasers actually have several longitudinal modes at the same time, and beats between the slightly different optical frequencies of those oscillations will in fact produce amplitude variations on time scales shorter than the round-trip time (the reciprocal of the frequency spacing between modes), typically a few nanoseconds or less. In most cases these lasers are still termed "continuous wave" as their output power is steady when averaged over any longer time periods, with the very high frequency power variations having little or no impact in the intended application.

For continuous wave operation, it is required for the population inversion of the gain medium to be continually replenished by a steady pump source. In some lasing media this is impossible. In some other lasers it would require pumping the laser at a very high continuous power level which would be impractical or destroy the laser by producing excessive heat. Such lasers cannot be run in CW mode.

1.6.2 PULSED OPERATION

Pulsed operation of lasers refers to any laser not classified as continuous wave, so that the optical power appears in pulses of some duration at some repetition rate. This encompasses a wide range of technologies addressing a number of different motivations. Some lasers are pulsed simply because they cannot be run in continuous mode.

In other cases the application requires the production of pulses having as large an energy as possible. Since the pulse energy is equal to the average power divided by the repetition rate, this goal can sometimes be satisfied by lowering the rate of pulses so that more energy can be built up in between pulses. In laser ablation for example, a small volume of material at the surface of a work piece can be evaporated if it is heated in a very short time, whereas supplying the energy gradually would allow for the heat to be absorbed into the bulk of the piece, never attaining a sufficiently high temperature at a particular point. Other applications rely on the peak pulse power (rather than the energy in the pulse), especially in order to obtain nonlinear optical effects. For a given pulse energy, this requires creating pulses of the shortest possible duration utilizing techniques such as Q-switching.

The optical bandwidth of a pulse cannot be narrower than the reciprocal of the pulse width. In the case of extremely short pulses, that implies lasing over a considerable bandwidth, quite contrary to the very narrow bandwidths typical of CW lasers. The lasing medium in some dye lasers and vibronic solid-state lasers produces optical gain over a wide bandwidth, making a laser possible which can thus generate pulses of light as short as a few femtoseconds (10−15 s).

1.6.3 Q-SWITCHING

In a Q-switched laser, the population inversion is allowed to build up by introducing loss inside the resonator which exceeds the gain of the medium; this can also be described as a reduction of the quality factor or 'Q' of the cavity. Then, after the pump energy stored in the laser medium has approached the maximum possible level, the introduced loss mechanism is rapidly removed or that occurs by itself in a passive device, allowing lasing to begin which rapidly obtains the stored energy in the gain medium. This results in a short pulse incorporating that energy, and thus a high peak power.

1.6.4 MODE LOCKING

A mode-locked laser is capable of emitting extremely short pulses on the order of tens of picoseconds down to less than 10 femtosecond. These pulses will repeat at the round trip time, that is, the time that it takes light to complete one round trip between the mirrors comprising the resonator. Due to the Fourier limit also known as energy-time uncertainty, a pulse of such short temporal length has a spectrum spread over a considerable bandwidth. Thus such a gain medium must have a gain bandwidth sufficiently broad to amplify those frequencies. An example of a suitable material is titanium-doped, artificially grown sapphire (Ti:sapphire) which has a very wide gain bandwidth and can thus produce pulses of only a few femtoseconds duration.

1.6.5 PULSED PUMPING

Another method of achieving pulsed laser operation is to pump the laser material with a source that is itself pulsed, either through electronic charging in the case of flash lamps, or another laser which is already pulsed. Pulsed pumping was historically used with dye lasers where the inverted population lifetime of a dye molecule was so short that a high energy, fast pump was needed. The way to overcome this problem was to charge up large capacitors which are then switched to discharge through flash lamps, producing an intense flash. Pulsed pumping is also required for three-level lasers in which the lower energy level rapidly becomes highly populated preventing

further lasing until those atoms relax to the ground state. These lasers, such as the excimer laser and the copper vapor laser, can never be operated in CW mode.

1.7 TYPES OF LASERS AND THERE OPERATING PRINCIPLES

Many materials can be used as the heart of the laser. Depending on the lasing medium lasers are classified as solid state and gas laser.

1.7.1 GAS LASERS

In gas lasers, as name suggests, the active laser medium is gas. Gaseous laser materials offer significant advantages over solid materials. Some of these advantages are:

- Gases act as homogeneous laser medium.
- Gases can be easily transported for cooling and replenishment.
- Gases are relatively inexpensive.

However, due to physical nature of gases (low densities), a large volume of gases is required to achieve the significant population inversion for laser action. Hence gas lasers used are relatively larger than solid state lasers. Some of the typical gas laser is:

Helium-neon, Argon, Carbon dioxide etc.

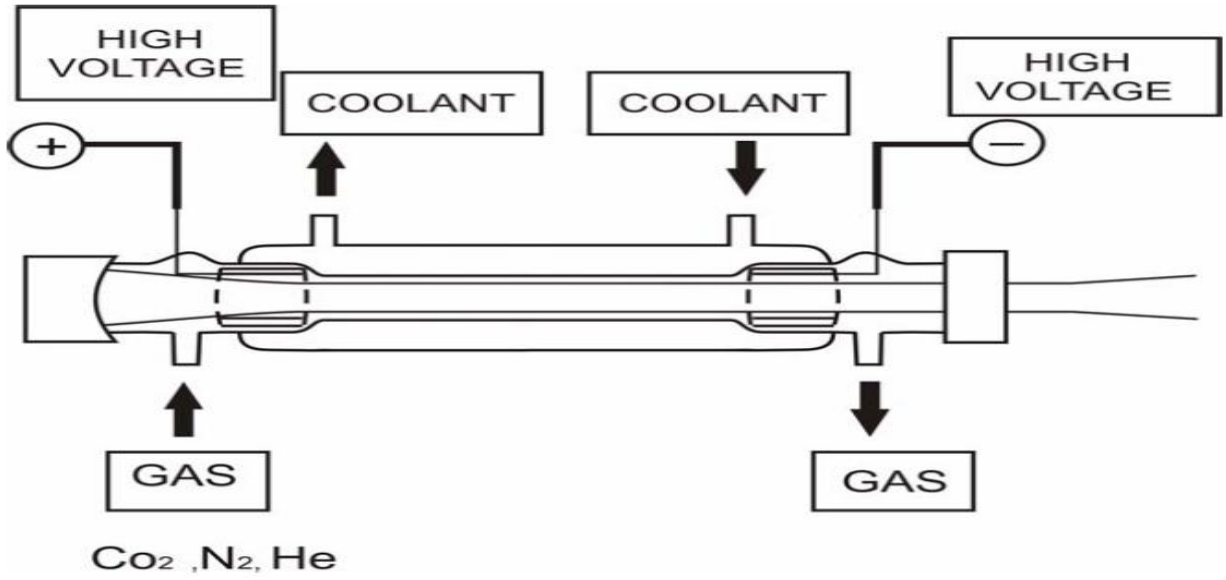

Fig. 1.7 Construction of a Co2 laser

(http://nptel.iitm.ac.in/courses/Webcourse-contents/IIT%20Kharagpur/Manuf%20Proc%20II/pdf/LM-40.pdf)

1.7.2 SOLID STATE LASERS

Solid-state lasers use a crystalline or glass rod which is doped with ions that provide the required energy states. For example, the first working laser was a ruby laser, made from ruby (chromium-doped corundum). The population inversion is actually maintained in the dopant, such as chromium or neodymium. These materials are pumped optically using a shorter wavelength than the lasing wavelength, often from a flashtube or from another laser.

It should be known that solid-state in this sense refers to a crystal or glass, but this usage is distinct from the designation of solid-state electronics in referring to semiconductors.

Semiconductor lasers (laser diodes) are pumped electrically and are thus not referred to as solid-state lasers. The class of solid-state lasers would, however, properly include fiber lasers in which dopants in the glass laser under optical pumping. But in practice these are simply referred to as fiber lasers with solid-state reserved for lasers using a solid rod of such a material.

Solid-state lasers are commonly of the following type:

- Ruby which is a chromium-alumina alloy having a wavelength of 0.7 micro-m.
- Nd-glass laser having a wavelength of 1.64 micro m.
- Nd-yag laser having a wavelength of 1.06 micro m.

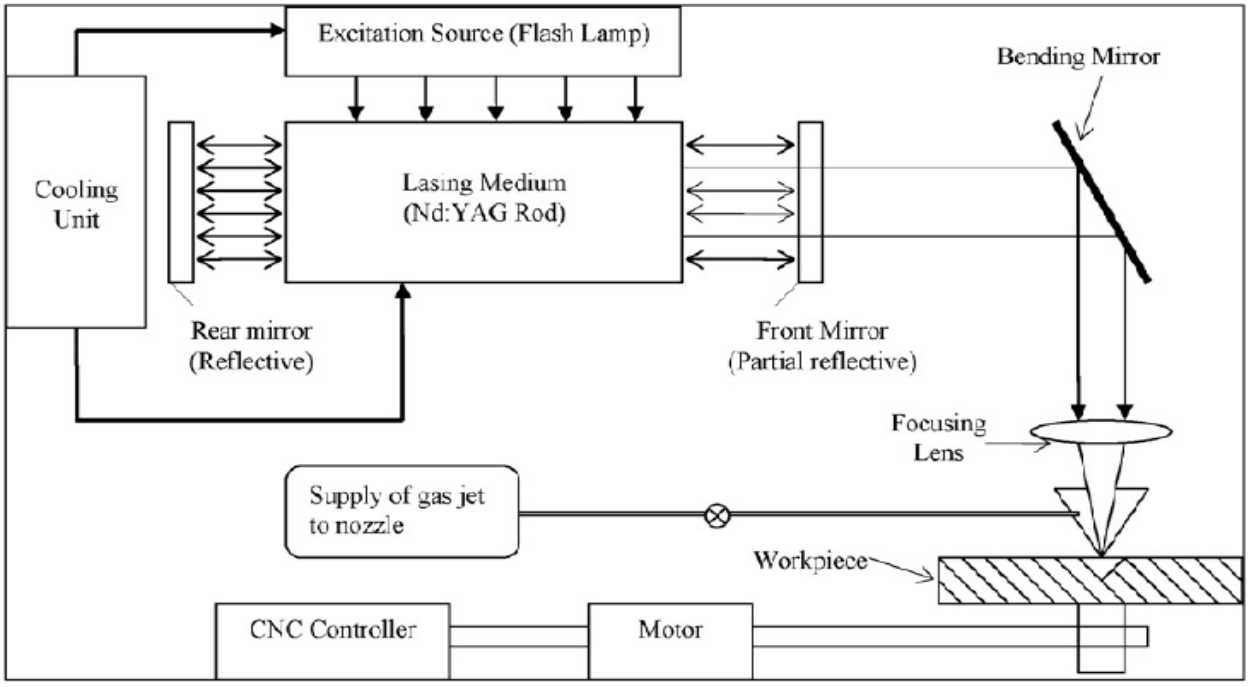

Fig. 1.8 Schematic of Nd: YAG laser beam cutting system (Dubey and yadava 2008)

1.7.3 FIBER LASERS

Solid-state lasers or laser amplifiers where the light is guided due to the total internal reflection in a single mode optical fiber are instead called fiber lasers. Guiding of light allows extremely long gain regions providing good cooling conditions; fibers have high surface area to volume ratio which allows efficient cooling. In addition, the fiber's wave guiding properties tend to reduce thermal distortion of the beam. Erbium and ytterbium ions are common active species in such lasers.

Quite often, the fiber laser is designed as a double-clad fiber. This type of fiber consists of a fiber core, an inner cladding and an outer cladding. The index of the three concentric layers is chosen so that the fiber core acts as a single-mode fiber for the laser emission while the outer cladding acts as a highly multimode core for the pump laser. This lets the pump propagate a large amount of power into and through the active inner core region, while still having a high numerical aperture (NA) to have easy launching conditions.

Fiber lasers have a fundamental limit in that the intensity of the light in the fiber cannot be so high that optical nonlinearities induced by the local electric field strength can become dominant and prevent laser operation and/or lead to the material destruction of the fiber. This effect is called photo darkening. In bulk laser materials, the cooling is not so efficient, and it is difficult to separate the effects of photo darkening from the thermal effects, but the experiments in fibers show that the photo darkening can be attributed to the formation of long-living color centers Fiber lasers have a fundamental limit in that the intensity of the light in the fiber cannot be so high that optical nonlinearities induced by the local electric field strength can become dominant and prevent laser operation and/or lead to the material destruction of the fiber. This effect is called photo darkening. In bulk laser materials, the cooling is not so efficient, and it is difficult to separate the effects of photo darkening from the thermal effects, but the experiments in fibers show that the photo darkening can be attributed to the formation of long-living color centers (Wikipedia, downloaded on 27/11/2012).

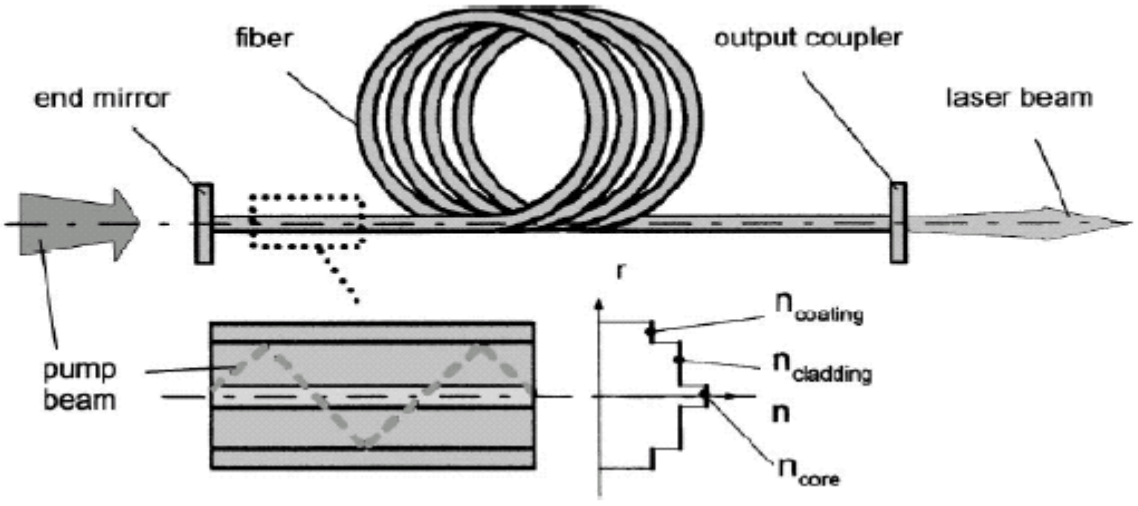

Fig. 1.9 Schematic of fiber lasers (Hugel, 2000).

1.7.4 CHEMICAL LASERS

Chemical lasers are powered by a chemical reaction permitting a large amount of energy to be released quickly. Such very high power lasers are especially of interest to the military; however continuous wave chemical lasers at very high power levels, fed by streams of gasses, have been developed and have some industrial applications.

1.7.5 EXCIMER LASERS

Excimer lasers are a special sort of gas laser powered by an electric discharge in which the lasing medium is an excimer, or more precisely an exciplex in existing designs. These are molecules which can only exist with one atom in an excited electronic state. Once the molecule transfers its excitation energy to a photon, therefore, its atoms are no longer bound to each other and the molecule disintegrates. This drastically reduces the population of the lower energy state thus greatly facilitating a population inversion. Excimers currently used are all noble gas compounds; noble gasses are chemically inert and can only form compounds while in an excited state. Excimer lasers typically operate at ultraviolet wavelengths with major applications including semiconductor photolithography and LASIK eye surgery. Commonly used excimer molecules

include ArF (emission at 193 nm), KrCl (222 nm), KrF (248 nm), XeCl (308 nm), and XeF (351 nm).The molecular fluorine laser, emitting at 157 nm in the vacuum ultraviolet is sometimes referred to as an excimer laser, however this appears to be a misnomer in as much as F_2 is a stable compound.

1.7.6 SEMICONDUCTOR LASERS

Semiconductor lasers are diodes which are electrically pumped. Recombination of electrons and holes created by the applied current introduces optical gain. Reflection from the ends of the crystal forms an optical resonator, although the resonator can be external to the semiconductor in some designs. Commercial laser diodes emit at wavelengths from 375 nm to 3500 nm. Low to medium power laser diodes are used in laser pointers, laser printers and CD/DVD players. Laser diodes are also frequently used to optically pump other lasers with high efficiency. External-cavity semiconductor lasers have a semiconductor active medium in a larger cavity. These devices can generate high power outputs with good beam quality, wavelength-tunable narrow-line width radiation, or ultra short laser pulses. Vertical cavity surface-emitting lasers (VCSELs) are semiconductor lasers whose emission direction is perpendicular to the surface of the wafer. VCSEL devices typically have a more circular output beam than conventional laser diodes, and potentially could be much cheaper to manufacture. Quantum cascade lasers are semiconductor lasers that have an active transition between energy sub-bands of an electron in a structure containing several quantum wells (Wikipedia, downloaded on 27/11/2012).

1.7.7 DYE LASERS

Dye lasers use an organic dye as the gain medium. The wide gain spectrum of available dyes, or mixtures of dyes, allows these lasers to be highly tunable, or to produce very short-duration pulses (on the order of a few femtosecond). Although these tunable lasers are mainly known in their liquid form, researchers have also demonstrated narrow-line width tunable emission in dispersive oscillator configurations incorporating solid-state dye gain media. In their most prevalent form these solid state dye lasers use dye-doped polymers as laser media.

1.8 PARAMETERS IN LASER BEAM CUTTING

Laser cutting is a process influenced by a large number of parameters. (J. R. Duflou, 2001). With a large number of the parameter, there are higher risks for a process to have higher error. The

error that occurred might disturbed the quality of a cutting process as well as the productivity of a process. With this problem in hand, lots of time, energy and cost required to overcome it. Even though there are problem in the process, the laser machining process still will become most demanding process for many company and factory because of the flexibility that it can provide.

In laser cutting, the cut surfaces also should be aware of parameters. The basic parameters in laser cutting are cutting speed, kerf width, and laser power, chemistry of gas, nozzle exit pressure, nozzle design, work piece thickness and surface quality. (B T. Rao, October 2002). These parameters need to be set by selecting the appropriate operating window of cutting speed, gas pressure, laser power and stand-off distance.

Laser types also play an important role in machining as much as the laser intensity because we obviously need a correct laser type for the certain process. For example, CO2 and Nd:YAG lasers is being used in machining, while, ultraviolet laser is being used in medical cutting application. (N. B. Dahotre, 2007). Each laser types can provide different application in machining. For melt transition process, the laser needed to use in the process is a laser emission characteristic that matched the material and machining dimensions. For surface vaporization process, laser with short pulses and higher power density may be used.

1.9 IMPORTANT CHARACTERISTIC PROPERTIES OF LASER CUT

The cut quality is determined by the amount of material removed and the material affected by the cutting process. The characteristic properties of the laser cut that are used to describe the cut quality include the kerf width, kerf deviation, perpendicularity of the cut edges, surface roughness, dross attachment and size of heat-affected zone (HAZ). The process parameters influence the efficiency of the laser cutting process and the quality of the cut edge obtained.

1.9.1 Kerf width

The kerf width refers to the width of the slot that is formed during through-thickness cutting and is normally narrower at the bottom surface of the work piece than at the top surface. The kerf width represents the amount of material removed during the cutting process, which is essentially wasted material; therefore, a smaller kerf width is always desirable especially when small details are to be cut.

1.9.2 Perpendicularity or angularity of the cut edges

The perpendicularity or squareness and inclination tolerance, u, is the greatest perpendicular distance between the actual surface and the intended surface as illustrated in figure . It is the sum of the angular deviation and the concavity or convexity of the surface.

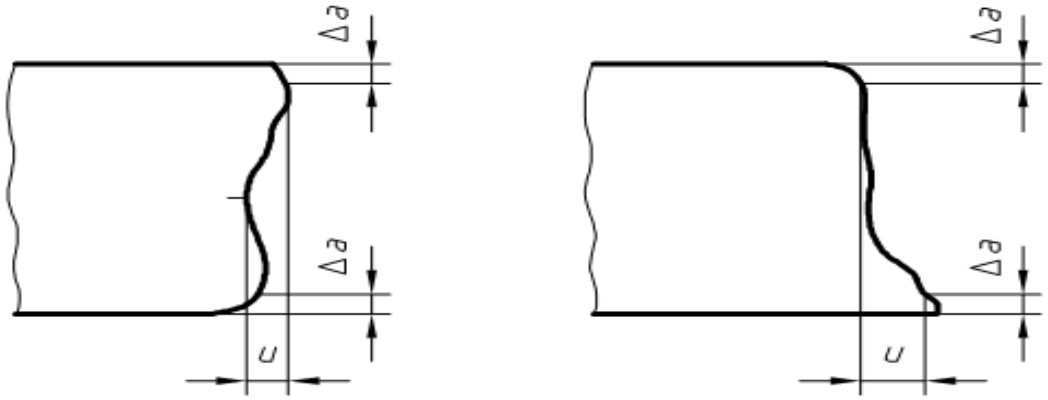

a) Vertical cut

Fig. 1.10 Perpendicularity tolerance of a straight laser cut, (Wandera, 2006)

Where U= Perpendicularity tolerance and a is thickness reduction for determination of U

1.9.3 Surface roughness

Surface roughness is the unevenness or irregularity of the surface profile and is measured as the mean height of the profile, R_z, or as an integral of the absolute value of the roughness profile, R_a. The mean height of the profile, R_z, is used in quality classification.

1.9.4 Dross attachment and burrs

A burr is the highly adherent dross (solidified material) or slag (solidified oxides) that forms on the underside of the cut. Molten materials with high values of surface tension and low viscosity are more difficult to remove from the cutting front by the assist gas and can result into adherent dross on the underside.

1.9.5 Heat Affected zone (HAZ) width

The thermal heat of laser cutting produces a heat affected zone (HAZ) next to the cut edge. The heat affected zone is the part of the material whose metallurgical structure is affected by heat but is not melted.

1.9.6 Kerf Deviation

The kerf deviation (Kd) is the difference of maximum and minimum width of top kerf measured along the length of cut.

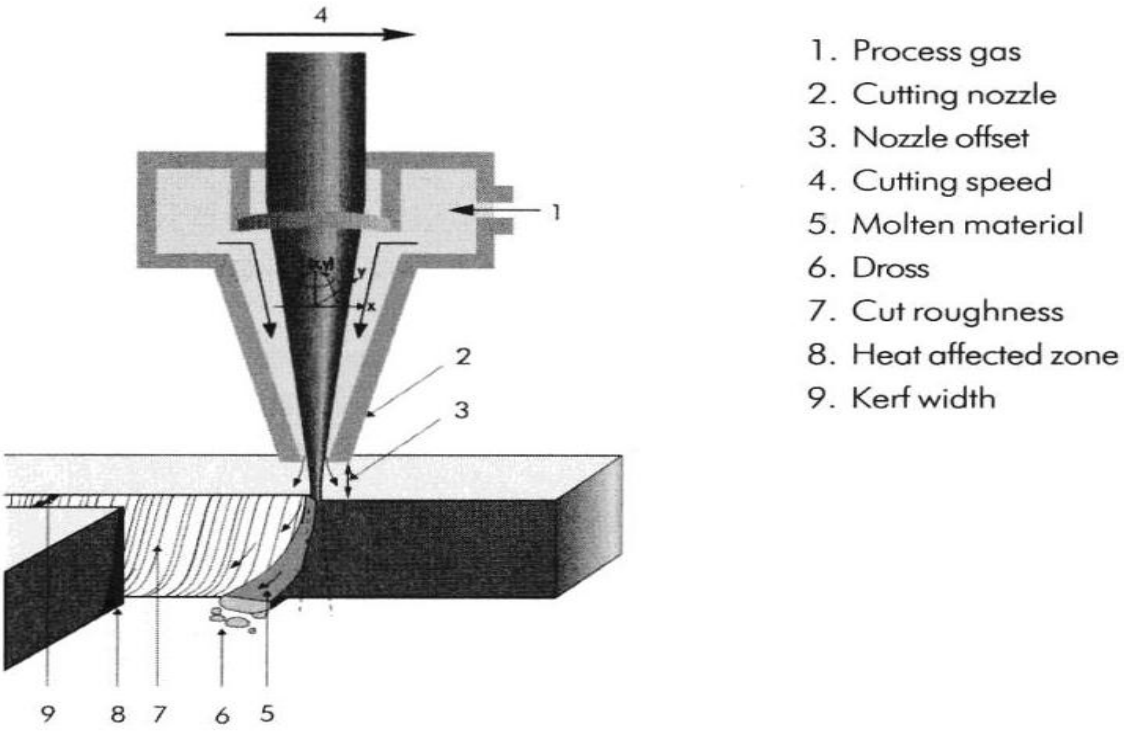

Fig. 1.11 Laser cut important surface characteristics, (Wandera, 2006)

1.10 APPLICATIONS

Fiber lasers have a wide range of applications and hence have the potential to dominate the material processing market in the future. These lasers are demonstrating process and cost advantages across the entire spectrum of material processing applications including: metal cutting, welding, silicon cutting, ceramic scribing, spot welding, bending, powder deposition, surface modification and marking. The applications by industry include:

- Automotive: welding transmission components, welding a sheet metal, cutting hydro-formed parts, marking, remote welding
- Computer: spot welding, annealing, silicon cutting

- Aerospace: welding Aluminum and Titanium, surface build up on blades, cutting aerospace components
- Medical device: marking, cutting, spot welding.

1.11 ADVANTAGES

Laser beam cutting is an advantageous technology choice. A careful evaluation of the features of the most suitable cutting system guarantees optimum results in the following aspects:

- Reduction of total work time
- Increase in production quality
- Laser cutting is precise, clean and silent.
- In laser cutting process, there is no physical tool. Thus no machining force or wear of the tool takes place.
- Though laser processing is a thermal processing but heat affected zone especially in pulse laser processing is not very significant due to shorter pulse duration.

The other ways beam can be localized on an extremely small area. The area in the proximity to the cut edge has a very low heat alteration. Moreover, the laser cut has the capacity of operating on complex profiles and with very small rays of curvature. Unlike water and other traditional cutting systems, light exerts no mechanical pressure on the piece. Moreover, laser is non contact instrument which guarantees:

- Total absence of mechanical pressure on work piece.
- Absence of wear in the instrument.
- Cutting capability independent of hardness of material.
- Capability of cutting coated or surface treated materials.

Laser cutting also has high degree of automation and flexibility able to offer the ease of integration with other automated systems, very high trimming capability and capability of adapting immediately to changes in production requirement.

1.12 LIMITATIONS

- High initial capital cost
- High maintenance cost
- Presence of heat affected zone-specially in gas assist co_2 laser cutting.
- Thermal Process, not suitable for heat sensitive materials like aluminium, glass, fiber.

Laser also has limitation capability on machining above two dimensional geometries compare to other machining methods. It means that in order to machine 3 dimensional and above level of geometries, suitable jigs and fixtures or special laser equipment laser systems are required to clamp work pieces.

CHAPTER 2
LITERATURE REVIEW

2.1 KERF GEOMETRY

Rajaram et al. (2003) conducted experiments on samples of 4130 steel with CO2 laser cutting system and the combined effects of power and feed rate on kerf width, surface roughness, striation frequency and heat affected zone have been studied. Regression analysis was used to develop models that describe the effect of the independent process parameters on laser cut quality. For the range of operation conditions tested, it was observed that power had a major effect on kerf width and size of HAZ, while feed rate affects were secondary. On the other hand, it was found out that surface roughness and striation frequency were affected most by feed rate.

Yilbas (2004) examined laser gas assisted cutting process and statistical method based on factorial analysis was introduced to identify the influence of cutting parameters on the resulting cut quality. International standards for thermal cutting were employed to identify the measurable variables when assessing the cut quality. Kerf width size was presented using scaling laws. Contribution of high temperature oxidation reaction in cutting due to assisting gas was accommodated in the analysis. An experiment was conducted to assess the cutting quality and validate the Kerf width predictions. It was found that increasing laser beam scanning speed reduced the Kerf width while Kerf width increased with increasing laser output power. The main effects of all the parameters employed had significant influence on the resulting cutting quality.

Karatas et al. (2006) conducted experiments on CO2 laser for cutting of steel and influence of beam waist position relative to the work piece surface and the work piece thickness on the striation formation was examined. The kerf width was modeled using a lump parameter analysis. The measurements are composed with the experimental findings. SEM and optical microscopy were conducted to examine the cutting surfaces. It was found that beam waist position had significant effect on the kerf size and as the work piece thickness reduces, the relative location of beam waist position varied for the minimum kerf width.

Dubey and yadava (2008) conducted experiments on nickel based super alloy (SUPERNI 718) sheet using Nd: YAG laser machine. A hybrid approach of Taguchi method (TM) and principal component analysis (PCA) had been applied for multi-objective optimization (MOO) of pulsed Nd:YAG laser beam cutting (LBC) to achieve better cut qualities within existing resources. The three-quality characteristics kerf width, kerf deviation (along the length of cut), and kerf taper had been considered for simultaneous optimization. Initially, single-objective optimization had been performed using Taguchi method and then the signal-to-noise (S/N) ratios obtained from Taguchi method had been further used in PCA for multi-objective optimization. The responses at predicted optimum parameter level were in good agreement with the results of confirmation experiments conducted for verification tests.

Sobih et al. (2008) presented the results of a laser cutting study using a 1 kW single-mode fibre laser, a relative newcomer in the field of laser metal cutting. Striation-free laser cuts were demonstrated when cutting 1mm thick mild steel sheets. The elimination of striation formation was considered important, since it could open a variety of novel high-precision applications. It was observed that the surface roughness decreased as the cutting speed increased until an optimum cutting speed was reached. Beyond this the surface roughness gradually increased again.

Powell et al. (2011) presented the results of an experimental and theoretical investigation into the phenomenon of 'striation free cutting', which is a feature of fibre laser/oxygen cutting of thin section mild steel. The author concluded that the creation of very low roughness edges was related to an optimization of the cut front geometry when the cut front was inclined at angles close to the Brewster angle for the laser– material combination. It was concluded by author that the lowest roughness mild steel cut edges are produced at intermediate speeds considerably lower than the maximum cutting speed.

Park et al. (2012) demonstrated an approach to improve laser machining quality on metals by vibrating the optical objective lens with a frequency (of 500Hz) and various displacements (0–16.5 mm) during a femtosecond laser machining process. The laser used in this experiment was an amplified Ti: sapphire fs laser system that generated 100fs pulses having energy of 3.5mJ/pulse with a 5 kHz repetition rate at a central wavelength of 790nm. It was found that both the wall surface finish of the machined structures and the aspect ratio obtained using the

frequency vibration assisted laser machining were improved, compared to those derived via laser machining without vibration assistance.

Rajpurohit and patel (2012) investigated and reviewed the striation mechanism which affect the quality of laser cutting and associated quality improvement techniques. Striation formation on the cut surfaces, which affects the surface roughness and geometry precision of laser cut product. An important weakness of this process is the formation of striations (regular lines down the cut surface), which affect the quality of the surfaces produced. It had been observed and found out by author that Control of striation could be achieved by stable melt flow from cutting front as well as intermediate cutting speed for a smooth cutting edge by optimization of the various process parameters like laser power, cutting speed and gas pressure which found out as major conflict the quality of cutting.

Stelzer et al. (2013) presented results of an experimental study on inert-gas fusion cutting of stainless steel with different types of laser. The cutting capabilities of a fiber and a CO2 laser beam with similar Rayleigh length had been compared as a function of material thickness with respect to achievable maximum cutting speed, cut edge surface roughness and cut kerf geometry. The author observed that the cut kerfs were nearly identical in size but differ qualitatively in shape for both laser types. Fiber and CO2 laser cutting results in AISI 304 stainless steel were compared. It was found out that a sudden increase in surface roughness is present at a particular sheet thickness. Under the defined experimental conditions, this transition occured between 4 and 6 mm in case of fiber laser cuts and between 8 and 10 mm for CO2 laser cutting trials. Furthermore, there were observed qualitative differences in the cut kerf shapes but with comparable kerf cross-section areas.

2.2 MRR

Dubey and yadava (2008) conducted experiments on Nd: YAG laser machine on thin sheet of high silicon alloy steel and presented a hybrid Taguchi method and response surface method (TMRSM) for the multi-response optimization of a laser beam cutting process. The approach used the Taguchi quality loss function to find the optimum level of input cutting parameters such as assist gas pressure, pulse width, pulse frequency and cutting speed. The optimum input parameter values were further used as the central values in the response surface method to develop and optimize the second-order response model. The two quality characteristics Kerf

width (KW), and material removal rate (MRR), that are of different nature (KW is of the smaller-the-better type, while MRR is of the higher the better type), had been selected for simultaneous optimization. This hybrid approach gave better quality results as compared to only Taguchi approach.

Dubey and yadava (2008) reviewed the experimental investigations carried out to study the effect of various factors/process parameters on the performance of Nd:YAG laser beam machining. The importance of different design of experiments (DOE) methodologies used by various investigators for achieving the optimum value of different quality characteristics were also discussed by them. They reviewed the different approaches used for experimental investigations on Nd:YAG laser beam cutting, drilling and micromachining of various materials such as metals, non-metals and composites. These investigations showed the effect of various factors on process performance and also the capabilities and applications of LBM. The variation of parameters and their effects on different quality characteristics were summarized into tables.

Sun et al. (2010) reviewed and summarized the up-to-date progress and benefits of thermally enhanced machining (with a focus on laser and plasma assistance) of ceramics, metals and metal matrix composites. They studied the integration of the external heat source with cutting tools, analysis of temperature distribution around the cutting region, material removal mechanisms, tool wear mechanisms and the improvement in machinability of various engineering materials by the assistance of external heat source. External heat sources were used to heat the work piece, and removed the work- piece locally in front of the cutting tool to facilitate the machining process by softening, change in deformation behavior and thinning of the work piece. It was found out by the authors, from previous researches, that the process lowered cutting forces, tool life increased, a better machined surface and higher material removal rate for a variety of work piece materials, such as ceramics, metals and composites. They also suggested about future works regarding: (1) Effective cooling of the cutting tool, (2) Application of the thermally enhanced machining to the ductile work piece, (3) Development of new heat sources.

Pandey and Dubey (2011) presented a modeling study of laser cutting process. A hybrid approach of Artificial Neural Network (ANN) and Fuzzy Logic (FL), Adaptive Neuro Fuzzy Inference System (ANFIS) had been used for developing the Kerf width and Material removal rate (MRR) models. The developed ANFIS based models of Kerf width and Material removal

rate were compared with Response Surface Methodology (RSM) based models and it was found that the values of Kerf width and Material removal rate predicted by the ANFIS based models were closer to the experimental values.

Ghosal and Manna (2012) conducted their experimental investigations on machining of Al/Al_2O_3-MMCby ytterbium fiber laser. The authors also explained the effects of different parameters on the response characteristics. The authors used response surface methodology for minimizing tapering and maximizing material removal rate. They developed mathematical models of higher order influences of various machining parameters such as laser power, modulation frequency, gas pressure, wait time on the tapering phenomena and material removal rate. Design of experiments was used to perform various experiments. The analysis of variance test has been performed to test the adequacy of the developed models for establishing the mathematical link between the response and the machining parameters of laser machining process. Response surfaces of taper and material removal rate were plotted with different parameters taken. It was concluded by authors that material removal rate increased with increase of N_2 gas pressure and range of the laser power was observed and noted during maximum material removal rate. The optimal parametric combination for maximized MRR and minimized taper was found out by them.

Kasashima et al. (2012) developed the experimental laser and electrochemical complex machining system for the On-machine measurement of the work piece position was performed using only one laser. On-machine measurement was used as one of the efficient methods to prevent the damage in the micro-fabrication, small installation misalignment and deformation of the work piece, which could cause fatal damage. Based on the measurement result, the position error of the work piece was automatically corrected and laser-machined. Electrochemical machining (ECM) was also done on the same machining system for the finishing purpose on that stent. They also explained the configuration of the system. Measurement and error correcting techniques were described in detail and the experimental results that made stent shape using the micro-tube of diameter 120 mm and210 mm were shown. The method to remove debris was not explained by authors.

Kang et al. (2012) conducted experiments by applying ultrasonic vibrations to a nanosecond laser machining process in order to improve the quality of machined surface. A resonance type

ultrasonic vibration module was designed to realize a unidirectional motion. To investigate the effects of ultrasonic vibration on the work surface, the morphological change of particles re-deposited on the machined area was observed in various process conditions. The results showed that the surface finish was improved by the near-field surface cooling enhancement induced by ultrasonic vibration. And it was found that such a vibration effect was remarkable in a repetitive machining process. From the chemical composition analysis of a machined surface, it was verified experimentally by them that the vibration can prevent the surface oxidation and the formation of recast layer. As a result, it was found by them that the ultrasonic vibration in ns-laser machining process was effective for improving both the physical and chemical quality of a machined surface.

2.3 OTHERS

Black et al. (1998) gathered the essential parameter information for the cutting of commercially-available ceramic tiles using a CO_2 laser cutting machine, with the object of producing a laser beam machining (LBM) database for their successful processing. Various laser cutting parameters were investigated that would generate a cut in ceramic tile which required minimal post-treatment. The effects of various shield gases, of multi pass cutting and of underwater cutting were also examined.

Hugel (2000) discussed some promising concepts based on different pumping techniques and crystal geometries, rods, discs, and fibers in view of attainable beam quality and means of power scaling. Disadvantages like poor beam quality and low efficiency were being effectively reduced by developments of diode-pumped systems. In the second part of the paper author presented investigations aimed at utilizing the beneficial properties of Nd: YAG-lasers, especially for welding. In particular, the advantages of the twin-focus technique were discussed in some detail with regard to power scaling, process improvements and flexibility increase. Based upon experience, the extension to a multi-focus technique was proposed by presenting experimental data obtained with lamp pumped high power lasers and results of numerical modelling. Author demonstrated the potential for industrial applications and provided an idea of what could be expected from the new generation of diode-pumped solid-state lasers with high beam quality.

Tsai et al. (2004) developed a new laser machining technique from the concept of fracture machining to produce a smooth surface of ceramic material. It involved the removal of a series

of small chip-elements. A focused laser generated micro-cracks on ceramic substrate, forming a fine crack network, then a defocused laser is scanned along the same path. The laser heat generated tensile stresses and induced the extension of the micro-cracks. Materials were removed due to the systematical linkage of the micro-cracks. The experimental material used was alumina ceramic and the laser source was CO_2 laser. The surface quality was found very well. The SEM photographs of the machining surface and the acoustic emission data were obtained to analyze the micro-mechanism of the fracture machining process. They investigated relationships between laser power, scanning speed, and chip-element size.

Pajak et al. (2004) conducted experiments by combining low power Laser beam machine with an electrolyte jet to make a hybrid process named Laser-assisted jet electrochemical machining (LAJECM). Compared to single jet electrochemical machining, LAJECM yielded better machining efficiency and precision, especially for small hole machining. The laser beam transferred additional heat on to a specific area of the work piece resulting in changed machining conditions. They also presented a mathematical modeling of the LAJECM process supported by experimental analysis.

Chang et al. (2007) conducted experiments to obtain different measures of surface roughness for Al2O3 work pieces which were machined by laser-assisted turning using a Nd:YAG laser. They analyzed the experimental results using the Taguchi method, which facilitated identification of optimum machining conditions. The findings indicated that rotational speed, with a contribution percentage as high as 42.68%, had the most dominant effect on LAM system performance, followed by feed, depth of cut, and pulsed frequency. They evaluated laser-assisted machining (LAM) as an economically viable process for manufacturing precision aluminum oxide ceramic parts, because it was locally heated by an intense laser source prior to material removal, LAM leads to higher material removal rates, as well as improved control of work piece properties and geometry. They measured and calculated material removal rate along with surface roughness. Using appropriately designed LAM experiments based on the Taguchi orthogonal array, they developed empirical models to evaluate the effects of the LAM process parameters and optimum operating conditions were found out by them.

Cicala et al. (2008) studied the limitations of laser machining of metals, and quantifies, through an experimental design method, the influence of operating parameters on productivity and on the

quality of the machined surface. Three study materials were used: an aluminium alloy, stainless steel and a titanium alloy. An initial reading of the results indicated that productivity depends mainly on the frequency of the laser pulse and that the aluminium alloy behaves differently from the other two. The quality of the machined surface was judged by roughness, was likewise dependent on pulse frequency and, to a lesser degree, on sweep speed. Surface roughness was minimized by increasing the pulse frequency and reducing the sweep speed. The experimental results were accurately predicted by simple polynomial models.

Jiao et al. (2008) proposed a dual-laser-beam method, where an off-focus CO_2 laser beam was used to preheat the glass sample to reduce the thermal gradients and a focused CO_2-laser beam was used to machine the glass. In the flat panel display (FPD) industry, lasers used to cut glass plates. In order to reduce the possibility of fracture in the process of cutting glass by lasers, the thermal stress has to be less than the critical rupture strength, so this technique was proposed. The distribution of the thermal stress and the temperature was simulated by using finite element analysis software, Ansys. The thermal stress was studied both when the glass sample was machined by a single CO_2-laser beam and by dual CO_2-laser beams. It was concluded by them that the thermal stress can be reduced by means of the dual-laser-beam method.

Hua et al. (2010) developed a process incorporating laser drilling with jet electrochemical machining (JECM-LD) to solve problems like recast layers and spatters that commonly accompanied laser drilled holes as well as to improve the overall quality of laser-drilled holes. It was executed by directing an electrolyte jet coaxially aligned with a laser beam onto the work piece surface. During the process, the electrolyte jet produced electrochemical reaction with the surface material, effective cooling of it and carried away the process scraps. A two-dimensional mathematical model was proposed to describe the shape of the holes machined by JECM-LD. The model was verified through comparison between the results from simulation and those from experiments conducted on the test pieces made of 321 stainless steel 0.5 mm thick processed by the pulsed Nd:YAG laser at second harmonic wavelength. It was evidenced that the JECM-LD that combines the laser drilling and jet electrochemical machining is on the position to obtain high machining quality with reduced recast layers and spatters. But its efficiency dropped by about 30%.

Yang et al. (2010) conducted an experimental study to characterize the heat affected zone produced when laser heating a Ti6Al4V alloy plate work piece. The emissivity and absorptivity of the Ti6Al4V alloy were determined experimentally. They developed a 3D transient finite element method for a moving Gaussian laser heat source to predict the depth and width of the heat affected zone on the Ti6Al4V alloy work piece. There was a close correlation between the experimental data and the simulation results. They found that the depth and width of the heat affected zone were strongly dependent on the laser parameters (laser power, laser scan speed, the angle of incidence and the diameter of the laser spot) and material properties (thermal conductivity, specific heat and density).They found out that the depth and width of the heat affected zone increased with an increase in the laser power and decreased with an increase of the laser spot size and the laser scan speed.

Stephen et al. (2010) conducted experiments by laser thermo chemical machining so that metallic micro parts can be produced with high quality when the etching liquid is injected coaxially to the laser beam directly into the irradiated area. The basic mechanisms and limits of the process were described. It was shown that the reaction is temperature driven, independent of the laser wavelength. A limiting factor was the diffusion of the anions, identified by comparing, experimentally determined and calculated diffusion coefficients for the reaction products. It was shown that the laser supported the kinematics of dissolution and had no melting effects because laser thermo chemical machining in a reactive fluid jet was driven by the temperature dependent proton activity of a redox reaction. The processing speed was limited by the diffusion of the anions formed during the redox reaction, in the case phosphate ions, from a certain depth of removal on. It was found experimentally that the radiation wavelength had an indirect influence by the differences in the absorptivity of the machined material, but no direct one. They also concluded that the machining quality with respect to aspect ratio, edge radius and roughness could be enhanced by increasing the velocity of the etching liquid.

Babic et al. (2011) investigated issues related to dicing and drilling of GaN-on-diamond wafers for RF power transistor applications using laser micromachining. Dicing and via drilling of GaN-on-diamond wafers to obtain clean shippable die presented a number of opposing constraints owing to phenomena specific to diamond processing: graphite debris deposition around the cut, cleaning of the debris, appearance of diamond dust during cleaving, and finally the speed of

wafer processing. The amount of graphite debris was controlled with the average laser power and oxygen concentration, and that it was efficiently cleaned, clearly favors performing wafer scribing (and subsequent processing) on the wafer level. Protecting the devices during via and scribing steps were essential. They explored laser dicing using 355 nm tripled Nd:YAG laser .They found that the etch rate was not very wavelength dependent, and confirmed that shorter pulses and reduced average laser powers lead to cleaner scribing.

Masood et al. (2011) Conducted experiments on laser-assisted machining of one such hard-to-wear materials, high chromium white cast iron, used in making heavy duty mineral processing equipment for the mining industry and presented results. In particular, the effect of laser on temperature, cutting forces, surface profile, hardness and cutting chips were presented. They observed from the chip formation that laser is causing more frequent shearing of material, less uniform surface formation, and the heat penetration increased as the distance between laser spot and tool increased. This lead to reduce the cutting forces with expected improvement in tool life. They found out from the results that laser-assisted machining of high chromium white cast iron showed potential to be a feasible alternative to hard machining of such materials.

Romoli et al. (2011) presented a model to estimate the main dimensions (depth and width) of the grooves produced by the laser on PMMA, taking into account the influence of the main process parameters (incident power, scanning speed and spot diameter). Co_2 laser machine was used for amorphous polymer (PMMA) as a flexible technique for the rapid fabrication of miniaturized structures such as micro fluidic devices. The theoretical model allowed to control the engraving process showing that laser could represent a valid alternative for the production of micro channels. PMMA single- use devices were found to be easier to manufacture with respect to the conventional glass or silicon products. In a second step, IR laser vaporization was adopted for the removal of a single layer of PMMA. This was achieved by using multiple overlapping sequences of straight grooves with different scanning directions. The proposed technique showed that the removal depth varied proportionally with the number of layers machined, while surface roughness was influenced by the grooves spacing and the orientation of the scanning direction between successive layers. A method for thermally bonding the PMMA sheets, constituting the 3D structure of the chip, was presented by them.

Darvishi et al. (2012) examined ultrafast laser machining of tapered micro channel trenches in both hard (soda–lime and borosilicate glasses) and soft (PDMS elastomer) transparent solids. A simple model for channel width and depth as a function of processing parameters and threshold fluence was presented by them. Estimated channel sizes from the model were in good agreement with experimental results. They also showed that the channel depth was a linear function of the number of laser pulses per channel width. All measurement data was found to collapse onto a single curve, which served as a useful guide for micromachining of tapered channels in transparent materials. The sample speed, number of passes, and laser power were varied, after which an optical microscope was used to assess the channel cross sectional geometry and dimensions. The relationship between channel geometry and processing parameters in general for non-Gaussian laser beam profiles was not explained by them.

2.4 LITERATURE SUMMARY

From the study of research papers on Laser Beam Machining, it is found that different kinds of laser beams have been used with different operating characteristics for improving MRR, kerf width, surface finish, striations affect etc. and different modifications are done for improving machining characteristics and these are found to be beneficial. Some are as:

1. Certain micro parts are produced with enhanced machining quality and roughness by thermo chemical machining.
2. Work has been done to reduce thermal stress produced in work material during cutting of material by using dual Co_2 laser beam machining.
3. MRR depends upon different type of laser beam machining equipment used with different operating characteristics.
4. Quality of drilled material of LCD glass by LBM can be increased when done under water than that of done in air.
5. Optimization of continuous wave Co_2 laser parameters have been done for maximum penetration and minimum heat input, width of heat affected zone in weldment.
6. Cutting speed of continuous wave Nd: YAG laser is found to be more than that of pulsed wave for cutting bare and coated metal plates.

7. Slow speed cutting causes no change in magnetic properties for average power of 100 W but magnetic flux density is found to be changed.
8. On machine measurement for the positioning of work piece three dimensionally is done to prevent it from misalignment and deformation.

2.5 GAPS IN LITERATURE REVIEW

Some gaps are identified on the basis of which aim for further study has been decided. Some are:

1. It has been seen that insufficient work has been done for optimization of fibre laser beam parameters for certain materials.

2. Surface finish enhancement needs to be done.

3. Most of the literature available in this area shows that researchers have concentrated on a single quality characteristic as objective during optimization of LBM.

CHAPTER 3

DESIGN OF STUDY AND EXPERIMENTATION

3.1 INTRODUCTION TO METHODOLOGY

In this section, methodology to do the work is explained in detail. Design of Experiment (DOE) technique will be used.

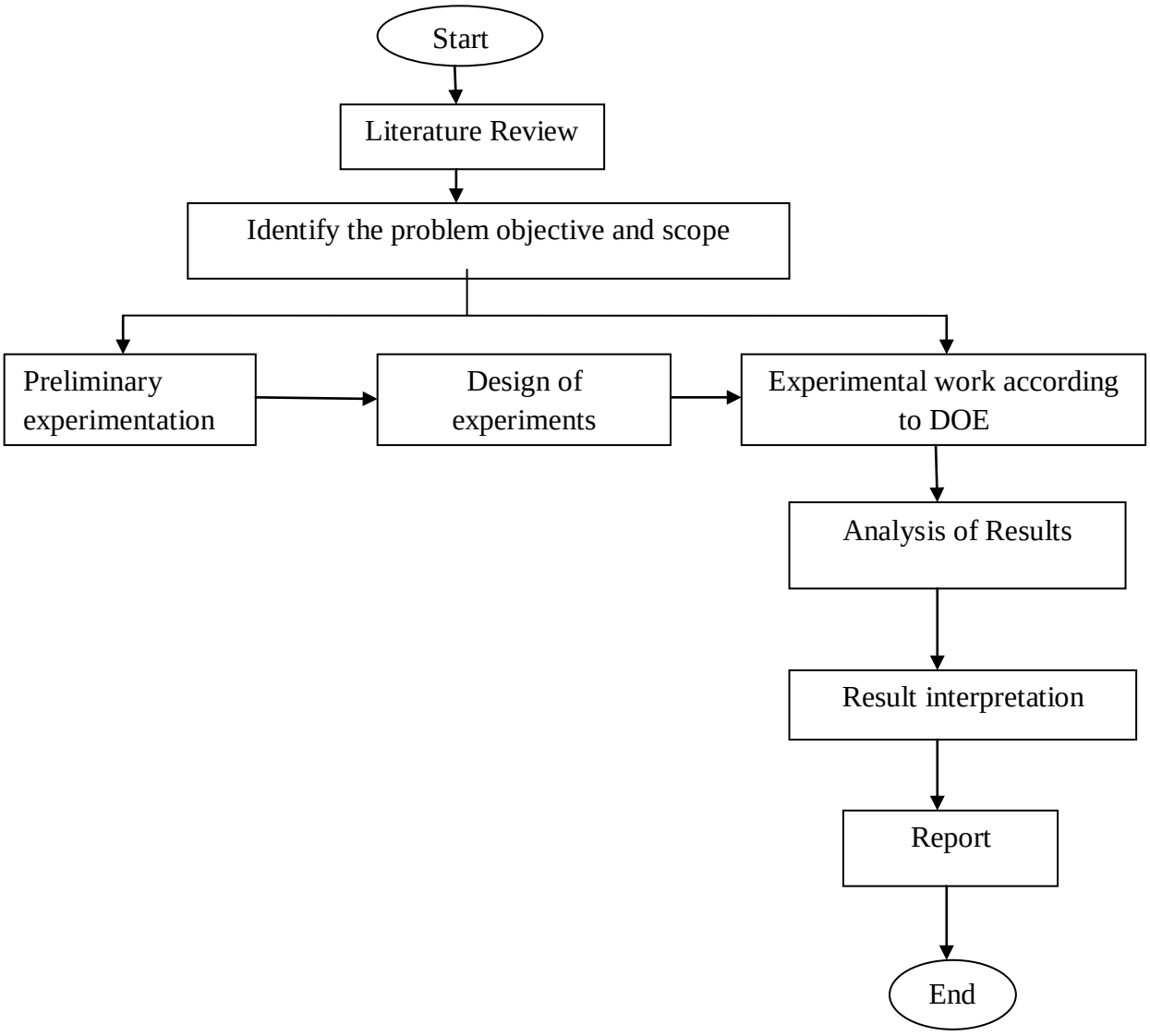

Figure 3.1: Flow chart of the experimentation

3.2 DESIGN OF EXPERIMENT (DOE)

It is a structured, organized method that is used to determine the relationship between the different factors affecting a process and the output of that process. This method was first developed in the 1920s and 1930, by Sir Ronald A. Fisher, the renowned mathematician and geneticist.

Design of Experiment involves designing a set of experiments, in which all relevant factors are varied systematically. When the results of these experiments are analyzed, they help to identify optimal conditions, the factors that most influence the results, and those that do not, as well as details such as the existence of interactions and synergies between factors. DOE methods require well-structured data matrices. When applied to a well-structured matrix, analysis of variance delivers accurate results, even when the matrix that is analyzed is quite small. Experimental design is a strategy to gather empirical knowledge, i.e. knowledge based on the analysis of experimental data and not on theoretical models. It can be applied whenever you intend to investigate a phenomenon in order to gain understanding or improve performance.

Design of Experiments (DOE) is widely used in research and development, where a large proportion of the resources go towards solving optimization problems. The key to minimizing optimization costs is to conduct as few experiments as possible. DOE requires only a small set of experiments and thus helps to reduce costs.

There are many types of design of experiments applied in research and development but out of which the most efficient and commonly used method of design of experiment is Taguchi that is used for the optimization process of various parameters.

3.2.1 Introduction to Taguchi method

The Taguchi method involves reducing the variation in a process through robust design of experiments. The overall objective of the method is to produce high quality product at low cost to the manufacturer. The Taguchi method was developed by Dr. Genichi Taguchi of Japan who maintained that variation. Taguchi developed a method for designing experiments to investigate how different parameters affect the mean and variance of a process performance characteristic that defines how well the process is functioning. The experimental design proposed by Taguchi involves using orthogonal

arrays to organize the parameters affecting the process and the levels at which they should be varies. Instead of having to test all possible combinations like the factorial design, the Taguchi method tests pairs of combinations. This allows for the collection of the necessary data to determine which factors most affect product quality with a minimum amount of experimentation, thus saving time and resources. The Taguchi method is best used when there are an intermediate number of variables (3 to 50), few interactions between variables, and when only a few variables contribute significantly.

3.2.1.1 Orthogonal arrays

Taguchi's orthogonal arrays are highly fractional designs, used to estimate main effects using only a few experimental runs. These designs are not only applicable to two level factorial experiments, but also can investigate main effects when factors have more than two levels. An orthogonal array is a type of experiment where the columns for the independent variables are "orthogonal" to one another. The Taguchi arrays can be derived or looked up. Small arrays can be drawn out manually; large arrays can be derived from deterministic algorithms. Generally, the arrays are selected by the number of parameters (variables) and the number of levels (states). Analysis of variance on the collected data from the Taguchi design of experiments can be used to select new parameter values to optimize the performance characteristic. The data from the arrays can be analyzed by plotting the data and performing ANOVA.

3.2.1.2 Taguchi Method Design of Experiments

The general steps involved in the Taguchi Method are as follows:

1. Define the process objective, or more specifically, a target value for a performance measure of the process. This may be a flow rate, temperature, etc. The target of a process may also be a minimum or maximum.
2. Determine the design parameters affecting the process. Parameters are variables within the process that affect the performance measure such as temperatures, pressures, etc. that can be easily controlled. The number of levels that the parameters should be varied at must be specified.

3. Create orthogonal arrays for the parameter design indicating the number of and conditions for each experiment. The selection of orthogonal arrays is based on the number of parameters and the levels of variation for each parameter.
4. Conduct the experiments indicated in the completed array to collect data on the effect on the performance measure.
5. Complete data analysis to determine the effect of the different parameters on the performance measure.

3.3 OBJECTIVE FUNCTION

The objective of the study is to evaluate the main effects of laser power, feederate, frequency and gas pressure on Material Removal Rate (MRR), Kerf Width (K_W) and Kerf Deviation (K_D). MRR was calculated using formula, KW and KD was measured by using profile projector equipment.

3.4 SELECTION OF PARAMETERS

The determination of which factors to investigate depends on responses of interest. The factors which affect responses were identified by brainstorming, trial experimentation and literature review. The list of factors studied with their levels is shown in the table 3.1.

Table 3.1 Factors and their levels

FACTORS		LEVELS	
	LEVEL-1	**LEVEL-2**	**LEVEL-3**
Feed rate (mm/min), A	150	300	450
Power (W), B	75	80	85
Gas pressure (Kg/cm^2), C	3	4	5
Frequency (Hz), D	50	60	70

The minimum degrees of freedom require in the experiment are the sum of all the degrees of freedom of factors. In the present experimental setup, all the four factors are kept at 3-levels. The number of degrees of freedom for all the four factors i.e. A, B, C and D are 2 each. The total degrees

of freedom for the experiment are 8 which are shown in the table 3.2. The most suitable orthogonal array that can be used for the experimentation is L9.

Table 3.2 Degree's of freedom of factors

FACTORS	A	B	C	D	TOTAL
Degrees of freedom	2	2	2	2	8

The 9 trial conditions represented by Taguchi's L9 are given in the table 3.3. The experimentation was done in the protected environment on mild steel sheet of 1 ft. * 1 ft. The experiments were repeated for 3 times to get more accuracy in the results.

Table 3.3 L9 EXPERIMETAL DESIGN

Trial no.	Feed rate (mm/min)	Power (W)	Frequency (Hz)	Pressure (Kg/cm^2)
1	150	75	50	3
2	150	80	60	4
3	150	85	70	5
4	300	75	60	5
5	300	80	70	3
6	300	85	50	4
7	450	75	70	4
8	450	80	50	5
9	450	85	60	3

3.5 EXPERIMENTAL SETUP

The experiments have been conducted on the Fiber Laser Beam Machine model PATRIOT 100 of Scantech Laser Pvt. Ltd. which is available at Thapar University, Patiala in Machine Tool Lab. It is a 100 W Fiber Laser with 1 ft. * 1 ft. CNC system fully integrated and with hardware, software and peripherals incorporated. It is a continuous mode laser beam machine having number of input parameters which could be varied i.e. laser power, frequency, feed rate, gas pressure, nozzle stand-off distance and type of gas used. Each parameter has its effect on the output parameters such as Material Removal Rate (MRR), Kerf Width (K_W) and Kerf Deviation (K_D). Laser Power, Frequency, Feed rate and Gas pressure were the parameters which were varied on machine for experimentation.

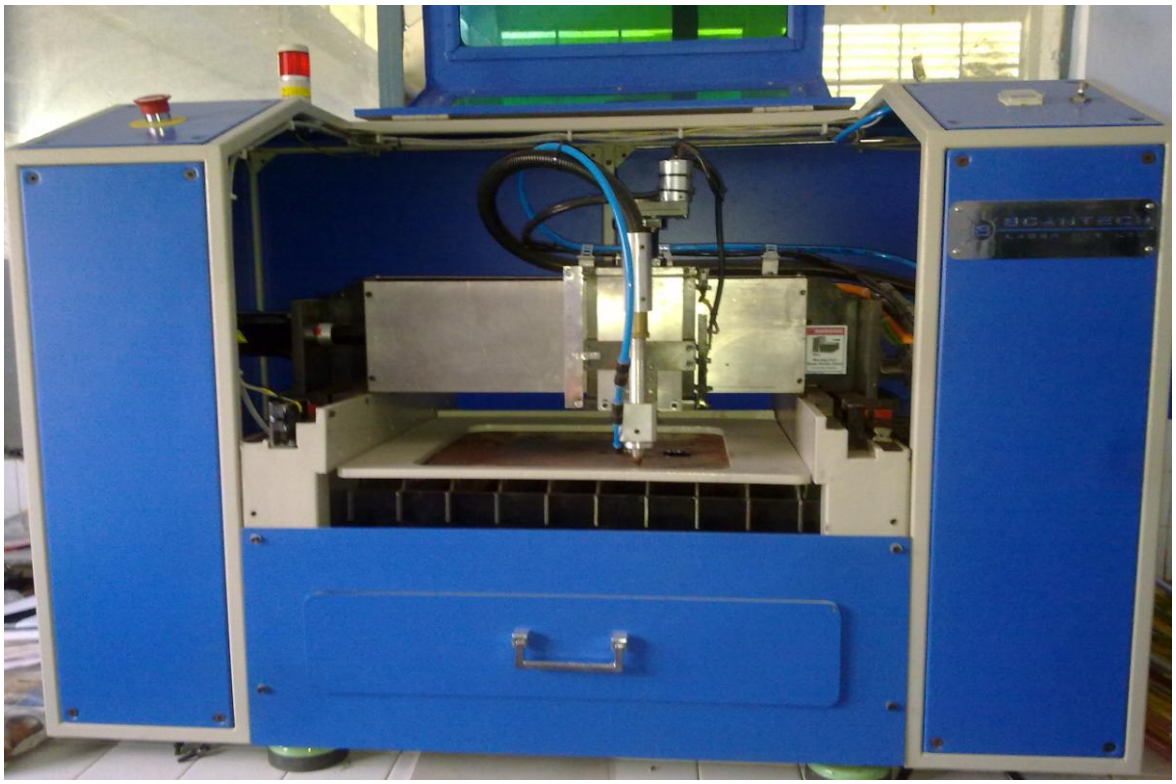

Fig. 3.2 Fiber Laser Beam Machine [Advanced machining lab, Thapar University]

The ranges of the values of these parameters for the experimental work have been selected on the basis of some trial experiments for which certain quality factors are taken care. The effect of these parameters has been checked on output factors like MRR, Kerf Width and Kerf Deviation. The factors which have been kept constant are given in table 3.4.

Table 3.4 Constant factors

S.No.	Parameters	Value/ Type
1	Stand-off distance	3 mm
2	Gas type	Oxygen
3	Material	M.S
4	Duty cycle	85%

Fig. 3.3 Control Unit of LBM [Advanced machining lab, Thapar University]

3.6 MEASURING AND TEST EQUIPMENT USED

Weighing machine, profile projector and spectrometer were used for measuring weight loss and calculating Material Removal Rate using that weight loss with formula, kerf width and composition of mild steel respectively. The details of important test equipment used in experimental study are given below as:

Weighing Machine

Weight difference of work piece before and after the performance trial was measured by weighing machine which was used further to calculated MRR. It has maximum limit of 500gm. and minimum limit is 200 mg.

Profile Projector

Measurement of Kerf Width and Kerf Deviation was measured on Nikon Profile Projector (Model: V-10A) of Japan which is available in Metrology Lab of Thapar University, Patiala. The voltage requirement is 220 V / 230 V / 240 V and current requirement is 0.6 A. Its least count is 0.001 mm.

Fig. 3.4 Profile Projector [Metrology lab, Thapar University]

Optical Emission Spectrometer

Chemical composition of the work piece base material is measured using Optical Emission Spectrometer Foundry Master (Model: DV-6), Baird, USA available at Thapar University, Patiala. An accuracy of 0.0001 % is achieved in the measurement. Argon gas is used for composition measurement process. It works by exciting atoms with energy that comes from a spark formed between the sample and electrode. The energy of the spark causes the electrons in the sample to emit light which is converted into a spectral pattern. By measuring the intensity of the peaks in this spectrum, OES analysers can produce materials composition.

Fig. 3.5 optical emission spectrometer [Material testing lab, Thapar University]

3.7 ANALYSIS OF RESULTS

Signal to noise ratio

The parameters that influence the output can be categorized into two classes, namely controllable (or design) factors and uncontrollable (or noise) factors. Controllable factors are those factors whose values can be set and easily adjusted by the designer. Uncontrollable factors are sources of variation often associated with operational environment. The best settings of control factors as

they influence the output parameters are determined through experiments. From the analysis point of view, there are three possible categories of the response characteristics explained below. *r* is the number of tests in a trial (noise of repetitions regardless of noise levels)

$\sum_{i=1}^{r}(y_i)^2$ = Summation of all response values under each trial

MSD = Mean square deviation

$Y_{i=}$ Observed value of the response characteristic

$Y_{0=}$ nominal or target value of the results

The three different response characteristics are given by the following.

1) Higher is better. The S/N for higher the better is given by:

$(S/N)_{HB} = -10 \log (MSD_{HB})$ Equation…..3.1

Where $MSD_{HB} = \frac{1}{r}\sum_{j=1}^{r}(\frac{1}{y_j})^2$ Equation…..3.2

MSD_{HB} = Mean Square Deviation for higher-the-better response.

2) Nominal is better. The S/N for nominal is better is:

$(S/N)_{NB} = -10 \log (MSD_{NB})$ Equation…..3.3

Where $MSD_{NB} = \frac{1}{r}\sum_{j=1}^{r}(y_j - y_0)^2$ Equation…..3.4

3) Lower is better. In this design situation, response is the type of ‘‘lower is better’’, which is a logarithmic function based on the mean square deviation (MSD), given by

$(S/N)_{LB} = -10 \log (MSD) = -10 \log [\frac{1}{r}\sum_{i=1}^{r}(y_i)^2]$ Equation…..3.5

Where $MSD_{LB} = \frac{1}{r}\sum_{j=1}^{r}(y_j)^2$ Equation……3.6

Signal to noise ratio for response characteristics

The parameters that influence the output can be categorized in two categories, controllable factors and uncontrollable factors. The control factors that may contribute to reduced variation can be quickly identified by looking at the amount of variation present in response. The

uncontrollable factors are the sources of variation often associated with operational environment. For this experimental work, response characteristics have given in the Table 3.5.

Table 3.5 Response Characteristics

Response Name	Response Type	Units
Material Removal Rate	Higher the better	mg/min
Kerf Width	Lower the better	mm
Kerf Deviation	Lower the better	mm

Measurement of F-value of Fisher's F ratio

The principle of the *F* test is that the larger the *F* value for a particular parameter, the greater the effect on the performance characteristic due to the change in that process parameter. *F* value is defined as:

$$F = \frac{MS\ for\ a\ term}{MS\ for\ the\ error\ term}$$

Equation ……3.7

Computation of average performance:

Average performance of a factor at certain level is the influence of the factor at this level on the mean response of the experiments.

Analysis of variance

The knowledge of the contribution of individual factors is critically important for the control of the final response. The analysis of variance (ANOVA) is a common statistical technique to determine the percent contribution of each factor for results of the experiment. It calculates parameters known as sum of squares (*SS*), pure *SS*, degree of freedom (DOF), variance, F-ratio and percentage of each factor. Since the procedure of ANOVA is a very complicated and employs a considerable of statistical formulae, only a brief description of is given as following.

The Sum of Squares (SS) is a measure of the deviation of the experimental data from the mean value of the data.

Let '*A*' be a factor under investigation

$$SS_T = \sum_{i=1}^{r} (y_i - \bar{\bar{T}})^2$$ Equation.……3.8

Where N = Number of response observations, T is the mean of all observations y_i is the i *th* response

Factor Sum of Squares (SS_A) - Squared deviations of factor (A) averages from overall average

$$SS_A = [\sum_{i=1}^{k_A} (\frac{\bar{\bar{A_i}}^2}{n_{Ai}})^1] - \frac{T^2}{N}$$ Equation …….3.9

Where

A_i =Average of all observations under A_i level = A_i/n_{Ai}

T = sum of all observations

$\bar{\bar{T}}$ = Average of all observations= T/N

n_{Ai} =Number of observations under A_i level

Error Sum of Squares (SS_e) - Squared deviations of observations from factor (A) Averages

$$SS_e = \sum_{j=1}^{k_A} \sum_{i=1}^{n_{Ai}} (y_i - \bar{A}_j)^2$$ Equation …….3.10

3.8 TEST RESULTS FOR WORK PIECE MATERIAL

Mild steel was used as the work piece for experimentation on fiber laser beam machine. Before the start of experimentation, the chemical composition of work piece material was measured on an Optical Emission Spectrometer DV-6. The percentage composition of the work piece material is provided in Table 3.6.

Table 3.6 Chemical Composition of Mild Steel

W/p	% Composition										
	Fe	C	Si	Mn	P	S	Co	Cu	Ti	W	Nb
MS	99.6	0.083	0.011	0.158	0.034	0.014	0.0035	0.0042	0.009	0.04	0.0054

3.8.1 Machined work pieces

Machined parts of mid steel sheets with laser cut are shown on the next three pages:

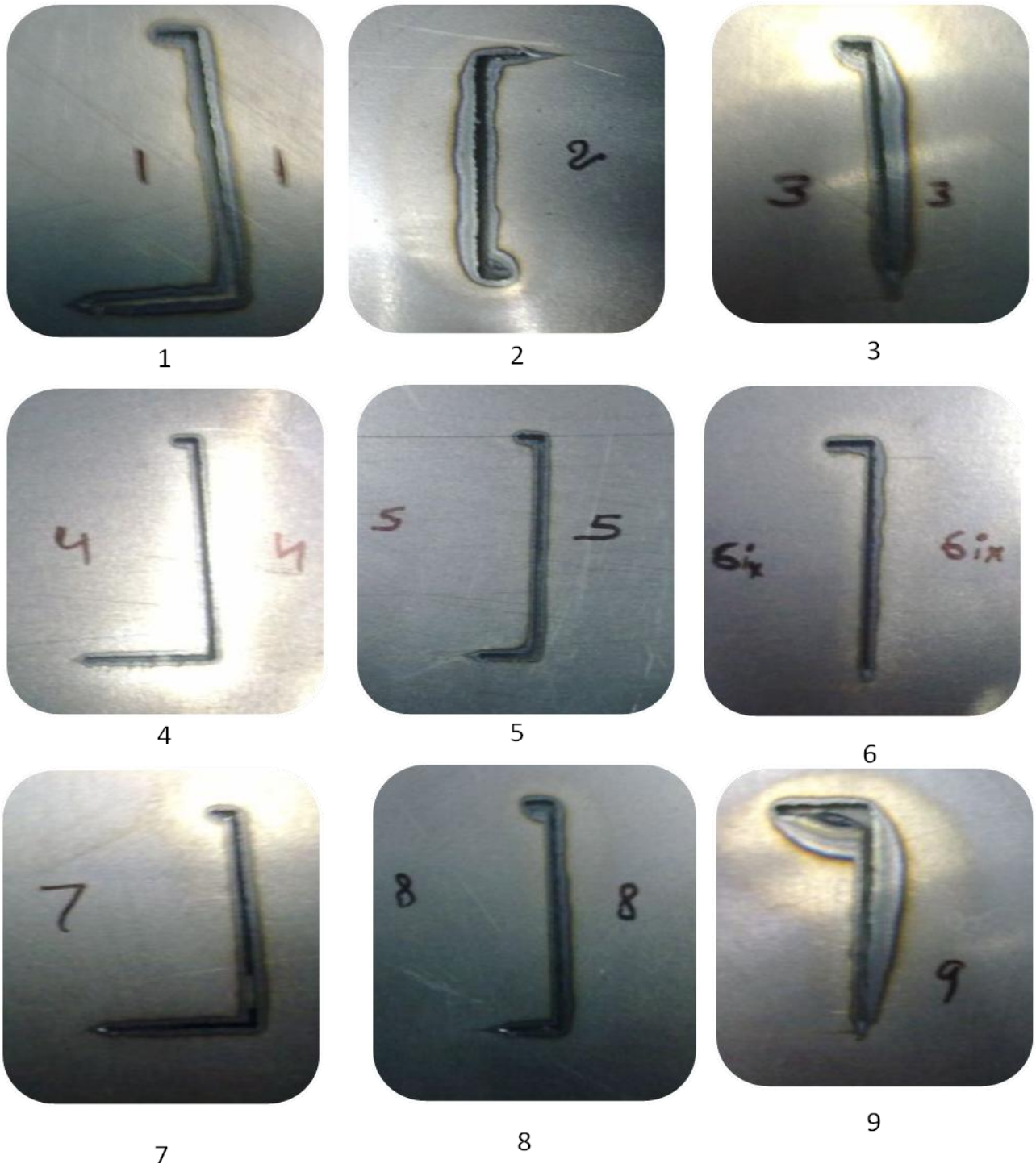

Fig. 3.6 Machined work pieces (trial 1)

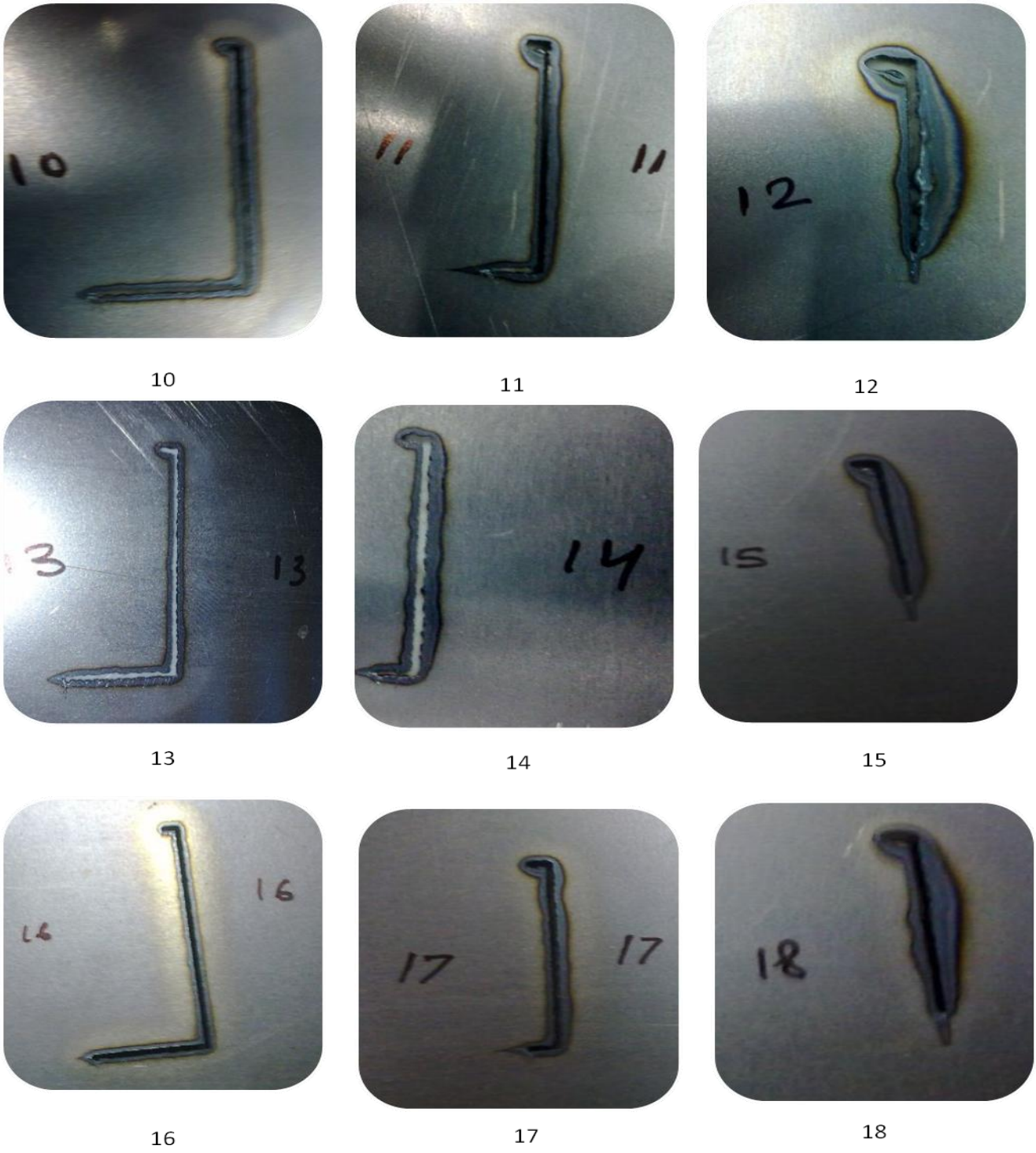

Fig. 3.7 Machined work pieces (trial 2)

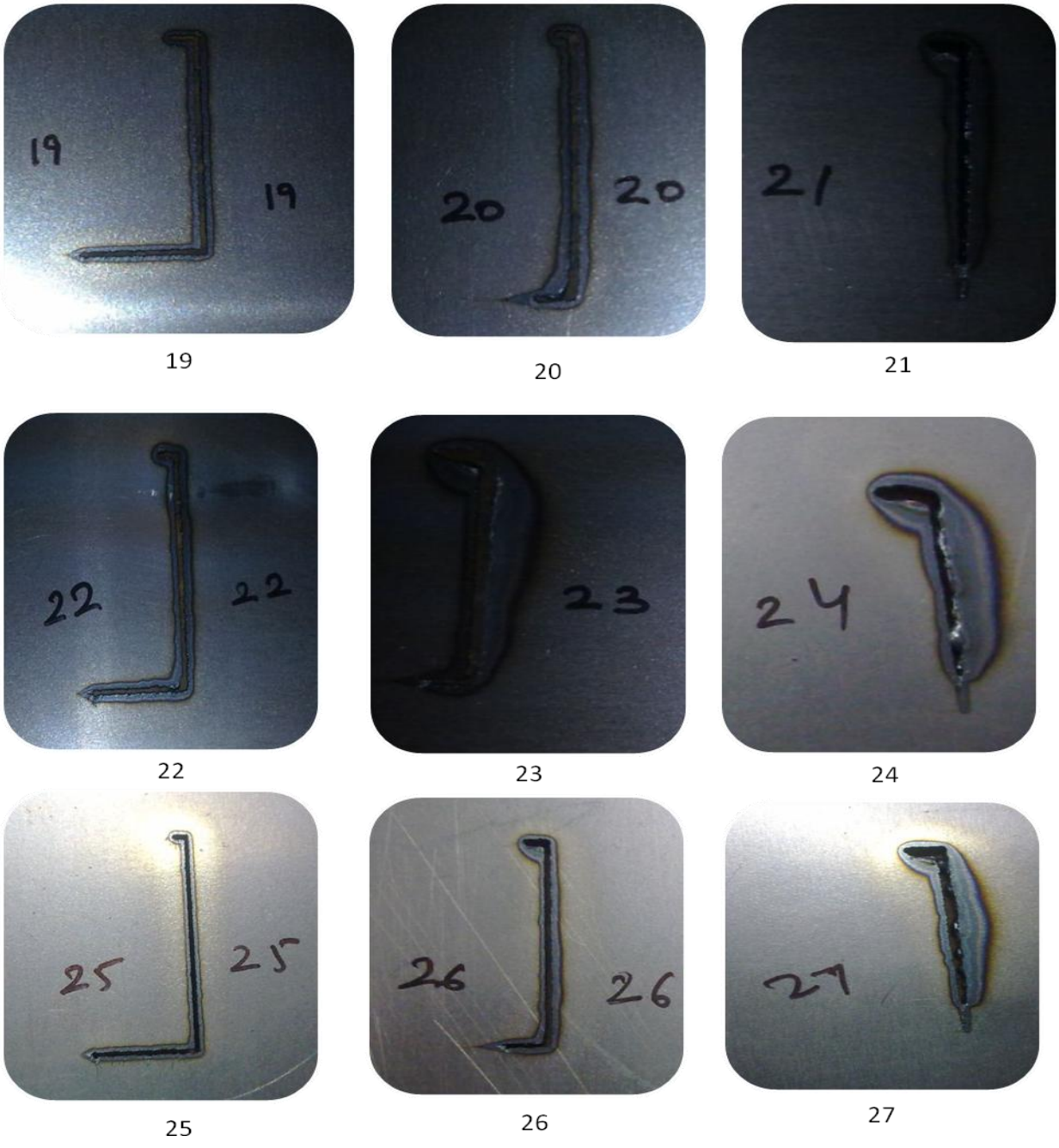

Fig. 3.8 Machined work pieces (trial 3)

CHAPTER 4

RESULTS AND ANALYSIS OF MRR

4.1 INTRODUCTION

The effects of parameters i.e. frequency, feed rate, power and gas pressure were evaluated using ANOVA. A confidence interval of 95 % has been used for the analysis. Three repetitions for each of 9 trails were completed to measure the Signal to Noise ratio(S/N Ratio).

4.2 RESULTS FOR MRR

The results for MRR for each of the 9 experiments with repetition are given in Table 4.1. MRR (mg/min) of each sample is calculated from weight difference of work piece before and after the performance trial, which is given by:

$$MRR = \frac{loss\ of\ mass\ during\ each\ cut \times cutting\ speed}{length\ of\ cut}$$

Equation ……4.1

Loss of mass during each cut is in mg

Cutting speed is in mm/min

Length of cut is in mm

Table 4.1: Results for MRR

Trial no.	Feed rate (mm/min.)	Power (W)	Frequency (HZ)	Pressure (Kg/cm^2)	MRR (mg/min.)			Mean MRR	S/N ratio
					1	2	3		
1	150	75	50	3	350.00	250.00	350.00	316.66	49.67
2	150	80	60	4	150.00	200.00	283.33	211.11	45.63
3	150	85	70	5	233.33	250.00	300.00	261.11	48.19
4	300	75	60	5	557.14	342.85	857.14	585.71	53.60

5	300	80	70	3	600.00	428.57	642.85	557.14	54.50
6	300	85	50	4	428.57	428.57	857.14	571.42	53.88
7	450	75	70	4	1050.0	600.00	450.00	700.00	55.41
8	450	80	50	5	707.14	525.00	375.00	535.71	53.71
9	450	85	60	3	385.71	750.00	1050.0	728.57	55.03

4.3 ANALYSIS OF VARIANCE – MRR

The results for MRR were analyzed using ANOVA for identifying the significant factors affecting the performance measures. The Analysis of Variance (ANOVA) for the mean MRR at 95% confidence interval is given in Table 4.2. The variance data for each factor was F-tested to find significance of each. The principle of the *F* test is that the larger the *F* value for a particular parameter, the greater the effect on the performance characteristic due to the change in that process parameter. ANOVA table shows that feed rate (F value 119.217) is the factor that significantly affects the MRR. All other factors namely, power, pressure and frequency are insignificant to affect the MRR. Table 4.3 shows the ranks of various factors in terms of their relative significance. Feed rate has the highest rank signifying highest contribution to MRR and frequency has the lowest and was observed to be insignificant in affecting MRR. Main effects plot for the MRR are shown in Figure 4.1 which shows the variation of MRR with the input parameters. As can be seen MRR increases with increase in feed rate from 105mm/min. to 450 mm/min. MRR is decreased when power increased from 75 W to 80 W and then increased with increase in power up to 85 W. MRR decrease with increase in pressure from 3 kg/cm^2 to 5 kg/cm^2.

Table 4.2: ANOVA for MRR

Source	DF	SS	MS	F	F-critical	% contribution
Feed rate	2	255601	127801	119.217	19	90.23
Power	2	17431	8715	8.126	19	6.15
Pressure	2	8077	4039	3.767	19	2.85
Error pooled(frequency)	2	2143	1072			0.76
Total	8	283253				

Table 4.3: Response table for means of MRR

Level	Feed rate (mm/min)	Power (W)	Frequency (Hz)	Pressure (kg/cm^2)
1	263	534.1	474.6	534.1
2	571.4	434.7	508.5	494.2
3	654.8	520.4	506.1	460.8
Delta	391.8	99.5	33.9	73.3
Rank	1	2	4	3

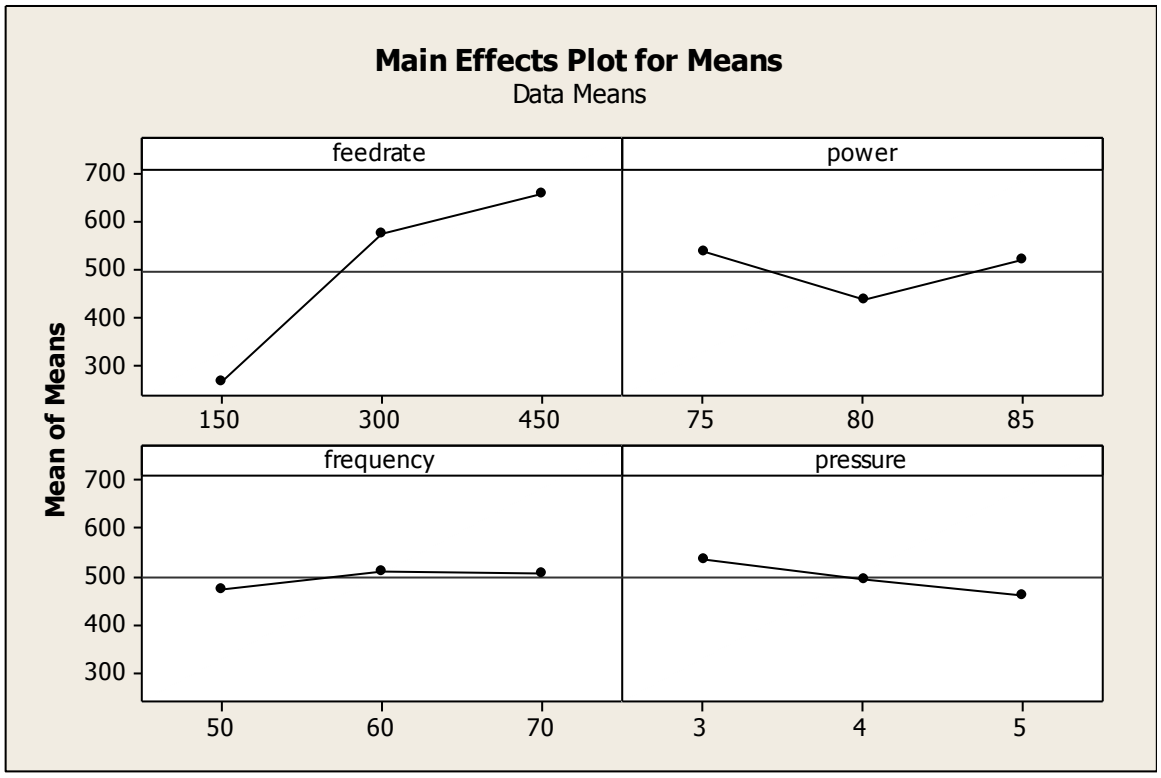

Figure 4.1: Main effects plot of MRR for Means

4.4 RESULTS FOR S/N RATIO OF MRR

The S/N ratio consolidates several repetitions into one value and is an indication of the amount of variation present. The S/N ratios have been calculated to identify the major contributing factors that cause variation in the MRR. MRR is "Higher is better" type response which is given by:

$(S/N)_{HB} = -10 \log (MSD_{HB})$ Equation…….4.2

Where $MSD_{HB} = \frac{1}{r}\sum_{j=1}^{r}\left(\frac{1}{y_j}\right)^2$ Equation…….4.3

MSDHB = Mean Square Deviation for higher the better response.

Table 4.4 shows the ANOVA results for S/N ratio of MRR at 95% confidence interval. Feed rate was observed to be the most significant factor affecting the MRR, followed by Power, according to F test. Main effects plot of S/N ratio for MRR are shown in the figure 4.2.

Table 4.4: ANOVA for S/N ratio of MRR

Source	DF	SS	MS	F-value	F-critical	% contribution
Feed rate	2	85.942	42.971	31.689	19	89.25
Power	2	4.051	2.025	1.493	19	4.21
Pressure	2	3.583	1.791	1.321	19	33.72
E-pooled (frequency)	2	2.712	1.356			2.82
Total	8	96.288				

Table 4.5: Response table for S/N ratio of MRR

Level	Feed rate (mm/min)	Power (W)	Frequency (Hz)	Pressure (kg/cm^2)
1	47.84	52.90	52.43	53.07
2	54.00	51.29	51.43	51.65
3	54.72	52.70	52.70	51.84
Delta	6.89	1.28	1.28	1.42
Rank	1	2	4	3

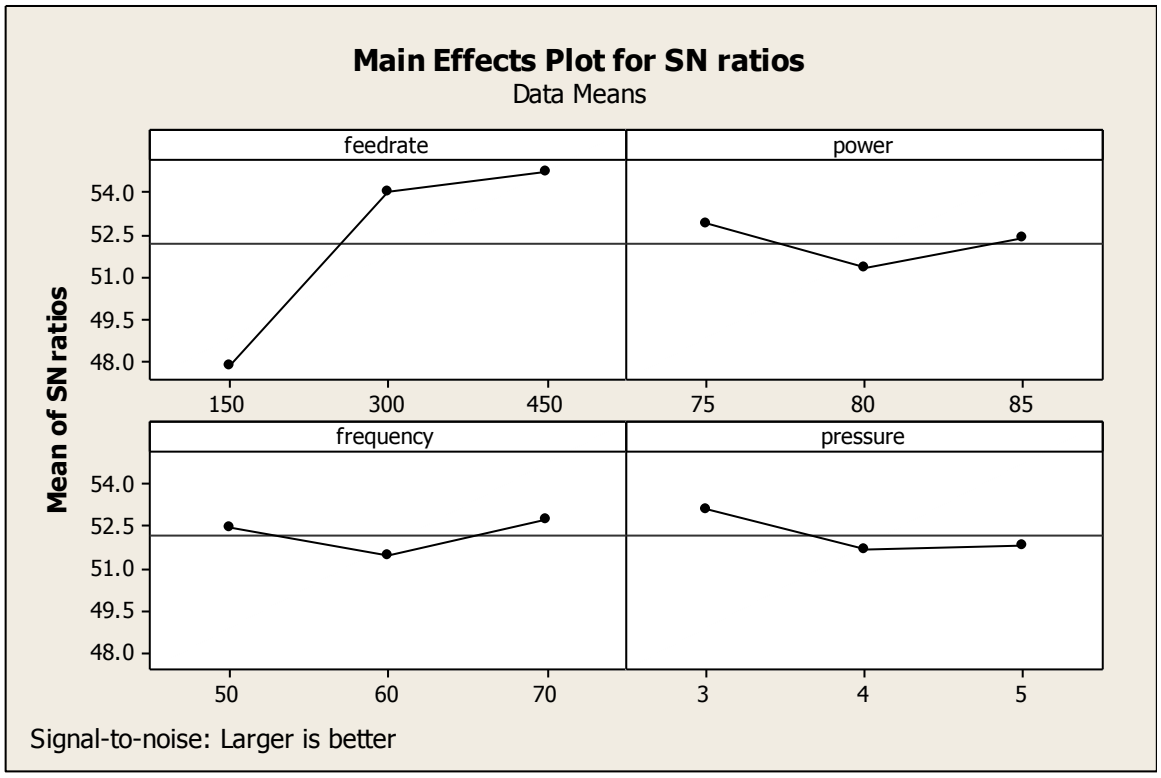

Figure 4.2: Main effects plot of MRR for S/N ratio

4.5 OPTIMAL DESIGN FOR MRR

The same level of all the significant factors provides a higher mean value and reduced variability so nothing has to be compromised. The level of factors which improves average and uniformity may conflict, so a compromise may have to be reached. Also a compromise has to occur when multiple responses are considered and the same factor level may cause one response to improve and other to deteriorate.

In this experimental analysis, the main effect plot in Figure 4.1 is used to estimate the mean MRR. From the Table 4.6, it is concluded that highest MRR was observed when material was machined at feed rate of 450 mm/min. out of the three levels. In S/N ratio highest MRR was observed when work piece material was machined at third level of feed rate i.e. 450 mm/min. The optimal values of means and S/N ratio are same, so there was no confliction according to their relative significance.

Table 4.6: Significant factors

Factor	Affecting mean		Affecting variance	
	Contribution	**Best level**	**Contribution**	**Best level**
Feed rate, A	significant	Level-3 (450mm/min.)	significant	Level-3 (450mm/min.)
Power, B	insignificant	-	insignificant	-
Gas pressure, C	insignificant	-	insignificant	-
Frequency, D	insignificant	-	insignificant	-

Estimating the mean foe MRR

In experimental analysis, the MRR is a higher average response is better (HB) characteristic. Depending on the characteristic, different treatment combinations has chosen to obtain satisfactory results. After conducting the experiments the optimum treatment condition within the experiments determined on the basis of prescribed combination of factor levels is determined to one of those in the experiment.

Mean value for MRR

$$\mu_A = A_3 - 0T \qquad \text{Equation…..4.4}$$

$$= 654.8 - 0 = 654.8 \text{mg/min}$$

Where T is given as mean MRR/no. of experiments

Confidence Interval around the Estimated Mean

The confidence interval is a maximum and minimum value between which the true average should fall at some stated percentage of confidence. The estimate of the mean μ is only a point estimate based on the averages of results obtained from the experiment. Statistically this provides a 50% chance of the true averages being greater than μ and a 50% chance of the true average being less than μ.

Confidence Interval around the estimated MRR mean

$$CI_1 = \sqrt{\frac{F_{\alpha,v_1,v_2} V_e}{\eta_{eff}}}$$ Equation…….4.5

Where $F_{\alpha\ v1\ v2}$ = F ratio

α = risk (0.05) confidence = 1-α

v_1 = degree of freedom for mean which is always = 1

v_2 = (Total degree's of freedom) - (degree's of freedom of significant factors)

V_e = (SS_{total}-$SS_{significant\ factors}$) / (total dof – dof of significant factors)

$$\eta_{eff} = \frac{N}{1+dof_A} = \frac{9}{1+2} = 3$$ Equation……..4.6

$$CI_1 = \sqrt{\frac{F_{\alpha,v_1,v_2} V_e}{\eta_{eff}}} = \sqrt{\frac{5.99 \times 4608.66}{3}} = 67.88$$

So the confidence interval around the MRR is given by 654.8±67.88 mg/min.

Confirmatory Results

Confirmatory experiments were conducted by taking the optimal values of all factors shown in the main effects plot of MRR for means i.e. feed rate (450 mm/min), power (75 W), frequency (60 Hz) and pressure (3 kg/cm^2).

Wt. of sample before machining = 471.41 gm

Wt. of sample after machining =471.36 gm

Wt. difference =0.05 gm, length of cut 35mm and cutting speed of 450 mm/min

MRR calculated by using the same formula given in equation no. 4.1. found to be 642.85 mg/min which was found to be in the range of calculated mean MRR.

CHAPTER 5

RESULTS AND ANALYSIS OF KERF WIDTH

5.1 INTRODUCTION

The effects of parameters i.e. frequency, feed rate, power and gas pressure were evaluated using ANOVA. A confidence interval of 95 % has been used for the analysis. Three repetitions for each of 9 trails were completed to measure the Signal to Noise ratio(S/N Ratio).

5.2 RESULTS FOR KERF WIDTH

The results for kerf width (K_W) for each of the 9 trials with 3 repetitions are given in Table 5.1. Kerf width of each cut has been measured at three different places at the top of the sheet. Average of these three measurements represents the kerf width of each cut. Kerf width was measured with the profile projector.

Table 5.1: Results for Kerf Width (K_W)

Trial no.	Feed rate (mm/min)	Power (W)	Frequency (Hz)	Pressure (kg/cm^2)	Kerf Width (mm)			Mean K_W	S/N ratio
					1	2	3		
1	150	75	50	3	0.588	0.555	0.659	0.600	4.404
2	150	80	60	4	0.604	0.512	0.558	0.558	5.047
3	150	85	70	5	0.561	0.530	0.612	0.567	4.902
4	300	75	60	5	0.473	0.688	0.722	0.627	3.913
5	300	80	70	3	0.310	0.578	1.080	0.656	2.739
6	300	85	50	4	0.857	0.705	0.602	0.721	2.746
7	450	75	70	4	0.700	0.844	0.854	0.799	1.911
8	450	80	50	5	0.427	0.819	0.728	0.658	3.362
9	450	85	60	3	0.728	1.009	1.092	0.943	0.392

5.3 ANALYSIS OF VARIANCE – KERF WIDTH

The results for kerf width were analyzed using ANOVA for identifying the significant factors affecting the performance measures. The Analysis of Variance (ANOVA) for the mean kerf width at 95% confidence interval is given in Table 5.2. The variance data for each factor were F-tested to find significance of each. ANOVA table shows that feed rate (F value 19.59) affect the kerf width and other factors like power (F value 5.569), pressure (F value 5.278) has little affect on kerf width. Frequency remains insignificant to affect K_W. It is observed that the feed rate is the most significant factor which contributes K_W followed by power and pressure with little affect. Main effects plot for K_W are shown in the Figure 5.1 that shows K_W increases with increase in feed rate from 105mm/min. to 450 mm/min. Table 5.3 shows ranks to various factors, feed rate has highest rank, most significant that affecting K_W.

Table 5.2: ANOVA for means of Kerf Width

Source	DF	SS	MS	F-value	F-critical	% contribution
Feed rate	2	0.0764	0.0382	19.59	19	62.32
Power	2	0.0217	0.0108	5.569	19	17.71
Pressure	2	0.0205	0.0102	5.278	19	16.78
E-pooled (frequency)	2	0.0039	0.0019			3.18
Total	8	0.1226				

Table 5.3: Response table for means of Kerf Width

Level	Feed rate (mm/min)	Power (W)	Frequency (Hz)	Pressure (kg/cm^2)
1	0.5754	0.6759	0.6600	0.7332
2	0.6683	0.6240	0.7096	0.6929
3	0.8001	0.7440	0.6743	0.6178
Delta	0.2247	0.1200	0.0496	0.1154
Rank	1	2	4	3

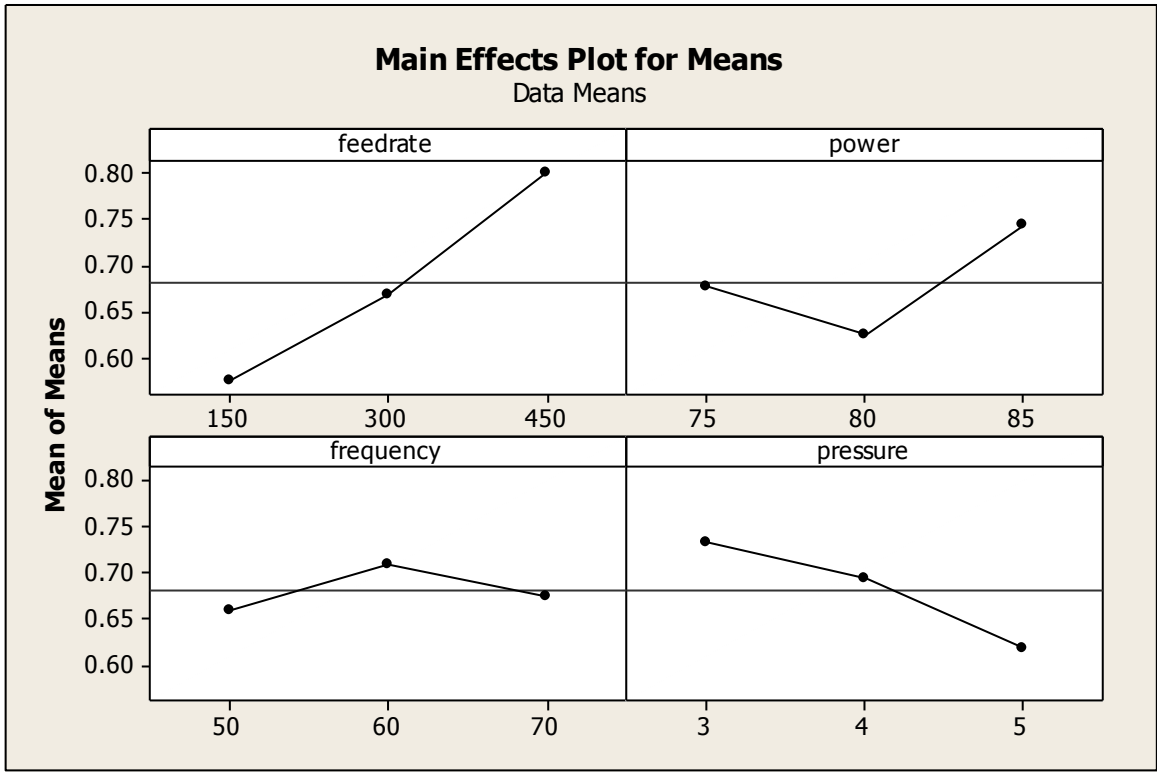

Figure 5.1: Main effects plot of Kerf width for Means

5.4 ANOVA FOR S/N RATIO FOR KERF WIDTH

The S/N ratio consolidates several repetitions into one value and is an indication of the amount of variation present. The S/N ratios have been calculated to identify the major contributing factors in the K_W. K_W is 'Lower is better' type response which is given by:

$$(S/N)_{LB} = -10 \log (MSD) = -10 \log \left[\frac{1}{r}\sum_{i=1}^{r}(y_i)^2\right] \quad \text{Equation……5.1}$$

Where $MSD_{LB} = \frac{1}{r}\sum_{j=1}^{r}(y_j)^2$ Equation……5.2

Table 5.4 shows the ANOVA for S/N ratio for KW at 95% confidence interval. The feed rate and pressure are the most significant in affecting Kerf width according to F test. Main effect plot of S/N ratios for Kerf width are shown in the Figure 5.3 and figure 5.4 respectively.

Table 5.4: ANOVA for S/N of Kerf Width

Source	DF	SS	MS	F-value	F-critical	% contribution
Feed rate	2	12.6623	6.3311	49.38	19	62.64
Power	2	1.6987	0.8493	6.62	19	8.403
Pressure	2	5.5966	2.7983	21.82	19	27.68
E-pooled (frequency)	2	0.2564	0.1282			1.268
Total	8	20.2140				

Table 5.5 Response table for S/N ratio of Kerf Width

Level	Feed rate (mm/min)	Power (W)	Frequency (Hz)	Pressure (kg/cm^2)
1	4.785	3.410	3.505	2.512
2	3.133	3.717	3.118	3.235
3	1.889	2.681	3.185	4.060
Delta	2.896	1.036	0.387	1.547
Rank	1	3	4	2

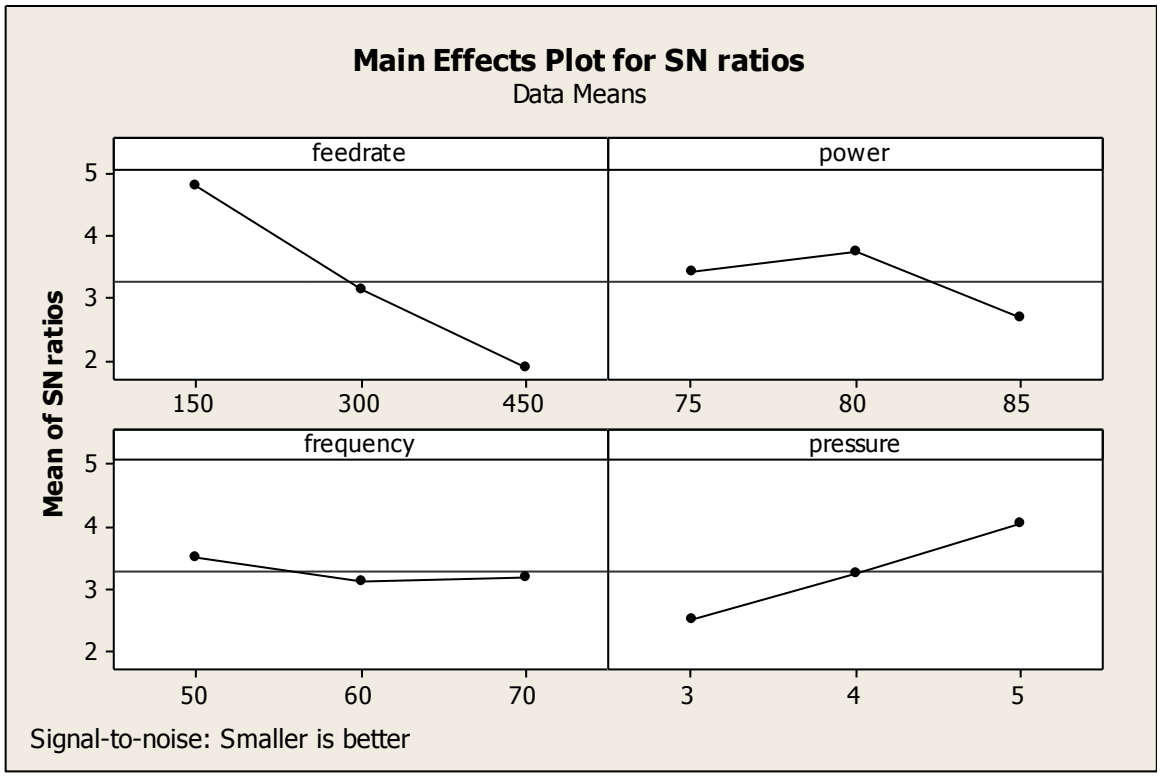

Figure 5.2 Main effects plot of K_W for S/N ratio

5.5 OPTIMAL DESIGN FOR KERF WIDTH

In this experimental analysis, the main effect plot in Figure 5.1 used to estimate the mean kerf width used to estimate the mean kerf width (K_W). From the Table 5.6, it is concluded that the lowest kerf width was to be observed when work piece was machined at feed rate of 150 mm/min i.e. level 1. Kerf width increased with increase in feed rate. In S/N ratio highest kerf width was to be observed when work piece material was machined at feed rate of 150 mm/min and gas pressure 5 kg/cm2 i.e. at level 3. So, best average value of K_W was suggested if work piece is machined at feed rate of 150 mm/min and with gas pressure 5 kg/cm^2.

Table 5.6 Significant factors

Factor	Affecting mean		Affecting variance	
	Contribution	**Best level**	**Contribution**	**Best level**
Feed rate, A	significant	Level-1 (150mm/min.)	significant	Level-3 (450mm/min.)
Power, B	insignificant	-	insignificant	-
Gas pressure, C	insignificant	-	significant	Level-3 (5 kg/cm^2)
Frequency, D	insignificant	-	insignificant	-

Estimating the mean foe kerf width

In experimental analysis, the kerf width is a lower average response is better (LB) characteristic. Depending on the characteristic, different treatment combinations has chosen to obtain satisfactory results. After conducting the experiments the optimum treatment condition within the experiments determined on the basis of prescribed combination of factor levels was determined to one of those in the experiment.

Mean value for Kerf Width

$$\mu_A = A_1 + C_3 - T \qquad \text{Equation…..5.3}$$

$$= 0.5754 + 0.6178 - 0.6812 = 0.512 \text{ mm}$$

Where T is given as mean K_W/no. of experiments

Confidence Interval around the Estimated Mean

The confidence interval is a maximum and minimum value between which the true average should fall at some stated percentage of confidence. The estimate of the mean μ is only a point estimate based on the averages of results obtained from the experiment. Statistically this provides a 50% chance of the true averages being greater than μ and a 50% chance of the true average being less than μ.

Confidence Interval around the estimated kerf width mean

$$CI_1 = \sqrt{\frac{F_{\alpha,v_1,v_2} V_e}{\eta_{eff}}}$$ Equation…….5.4

Where $F_{\alpha\ v1\ v2}$ = F ratio

α = risk (0.05) confidence = 1-α

v_1 = degree of freedom for mean which is always = 1

v_2 = (Total degree's of freedom) - (degree's of freedom of significant factors)

V_e = (SS_{total}-$SS_{significant\ factors}$) / (total dof – dof of significant factors)

$$\eta_{eff} = \frac{N}{1 + dof_{A,c}} = \frac{9}{1+2+2} = 1.8$$ Equation……..5.5

$$CI_1 = \sqrt{\frac{F_{\alpha,v_1,v_2} V_e}{\eta_{eff}}} = \sqrt{\frac{7.71 \times 0.0064}{1.8}} = 0.165$$

So the confidence interval around the kerf width (K_W) is given by 0.512±0.165 mm.

Confirmatory Results

Experiments were conducted by taking optimal values of all factors as shown in the main effects plot of kerf width for means, i.e. feed rate (150 mm/min), power (80W), gas pressure (5 kg/cm^2) and frequency (50 Hz).

Mean of the three values taken i.e. (0.457, 0.635 and 0.524) for the kerf width came out as 0.538mm, which is within the range.

CHAPTER 6

RESULTS AND ANALYSIS OF KERF DEVIATION

6.1 INTRODUCTION

The effects of parameters i.e. frequency, feed rate, power and gas pressure were evaluated using ANOVA. A confidence interval of 95% has been used for the analysis. Three repetitions for each of 9 trails were completed to measure the Signal to Noise ratio(S/N Ratio).

6.2 RESULTS FOR KERF DEVIATION (K_D)

The results for K_D for each of the 9 trials with 3 repetitions are given in Table 6.1. The kerf deviation is the difference of maximum and minimum width of top kerf measured along the length of cut. K_D was measured by the profile projector. It's measured in mm.

K_D =maximum top kerf width- minimum top kerf width.

Table 6.1: Results for Kerf Deviation

Trial no.	Feed rate (mm/min)	Power (KW)	Frequency (Hz)	Pressure (kg/cm^2)	Kerf deviation (mm)			Mean KD	S/N ratio
					1	2	3		
1	150	75	50	3	0.307	0.329	0.356	0.330	9.596
2	150	80	60	4	0.380	0.373	0.157	0.303	9.883
3	150	85	70	5	0.305	0.264	0.237	0.268	11.369
4	300	75	60	5	0.217	0.322	0.384	0.307	10.025
5	300	80	70	3	0.300	0.285	0.736	0.440	6.240
6	300	85	50	4	0.428	0.342	0.355	0.375	8.475
7	450	75	70	4	0.255	0.495	0.832	0.527	4.761
8	450	80	50	5	0.399	0.517	0.594	0.503	5.854
9	450	85	60	3	0.632	0.674	0.581	0.629	4.011

6.3 ANALYSIS OF VARIANCE- KERF DEVIATION

The results for kerf deviation were analyzed using ANOVA for identifying the significant factors affecting the performance measures. The Analysis of Variance (ANOVA) for the mean K_D at 95% confidence interval is given in Table 6.2. The variance data for each factor were F-tested to find significance of each. ANOVA table shows that feed rate (F value 526.3) and pressure (F value 90.42) are factors that affect the K_D. It is observed that the feed rate is the most significant factor followed by pressure. Power has little affected on K_D. Main effects plot for K_D are shown in the Figure 6.1 that shows K_D increases with increase in feed rate. K_D decreases as pressure increases from 3 kg/cm^2 to 5 kg/cm^2.

Table 6.2: ANOVA for means of Kerf Deviation

Source	DF	SS	MS	F-value	F-critical	% contribution
Feed rate	2	0.1010	0.0505	526.3	19	83.73
Power	2	0.0020	0.0010	10.83	19	1.72
Pressure	2	0.0173	0.0086	90.42	19	14.38
E-pooled (frequency)	2	0.0001	0.00009			0.15
Total	8	0.1207				

Table 6.3: Response table for means of Kerf Deviation

Level	Feed rate (mm/min)	Power (W)	Frequency (Hz)	Pressure (Kg/cm^2)
1	0.3009	0.3886	0.4030	0.4667
2	0.3743	0.4157	0.4133	0.4019
3	0.5532	0.4242	0.4121	0.3599
Delta	0.2523	0.0357	0.0103	0.1068
Rank	1	3	4	2

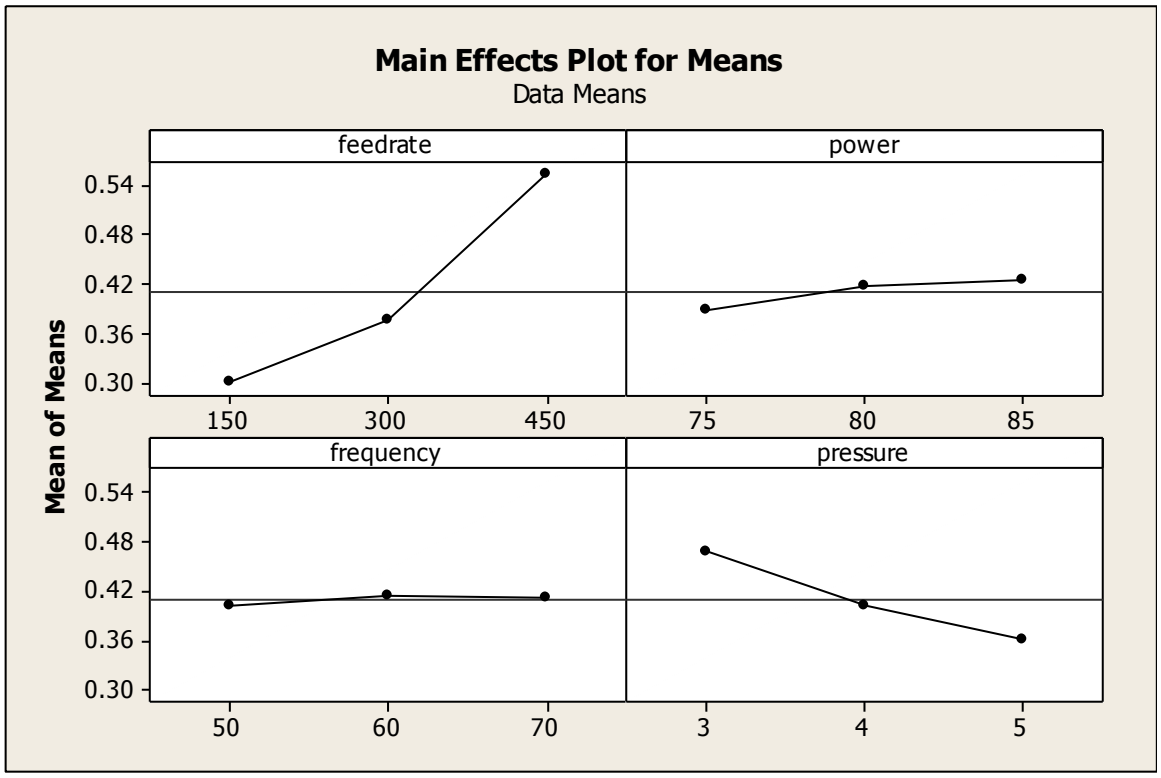

Figure 6.1 Main effects plot of Kerf Deviation for means

6.4 ANOVA FOR S/N RATIO FOR KERF DEVIATION (K_D)

The S/N ratio consolidates several repetitions into one value and is an indication of the amount of variation present. The S/N ratios have been calculated to identify the major contributing factors that cause variation in the K_D. K_D is 'Lower is better' type response which is given by:

$$(S/N)_{LB} = -10 \log (MSD) = -10 \log \left[\frac{1}{r} \sum_{i=1}^{r} (y_i)^2 \right] \quad \text{Equation……6.1}$$

Where $MSD_{LB} = \frac{1}{r} \sum_{j=1}^{r} (y_j)^2$ Equation……6.2

Table 6.4 shows the ANOVA for S/N ratio for K_D at 95% confidence interval. The feed rate is the most significant factor affecting K_D according to F test. Main effect plot of S/N ratios for K_D are shown in the Figure 6.2.

Table 6.4: ANOVA for S/N of Kerf Deviation

Source	DF	SS	MS	F-value	F-critical	% contribution
Feed rate	2	44.7512	22.3756	83.61	19	80.60
Power	2	1.0654	0.5327	1.9906	19	1.918
Pressure	2	9.1687	4.5843	17.13	19	16.514
E-pooled (frequency)	2	0.5351	0.2676			0.96
Total	8	55.5204				

Table 6.5 Response table for S/N ratio of Kerf Deviation

Level	Feed rate (mm/min)	Power (W)	Frequency (Hz)	Pressure (Kg/cm^2)
1	10.283	8.128	7.975	6.616
2	8.247	7.326	7.973	7.707
3	4.876	7.952	7.457	9.083
Delta	5.407	0.802	0.518	2.467
Rank	1	3	4	2

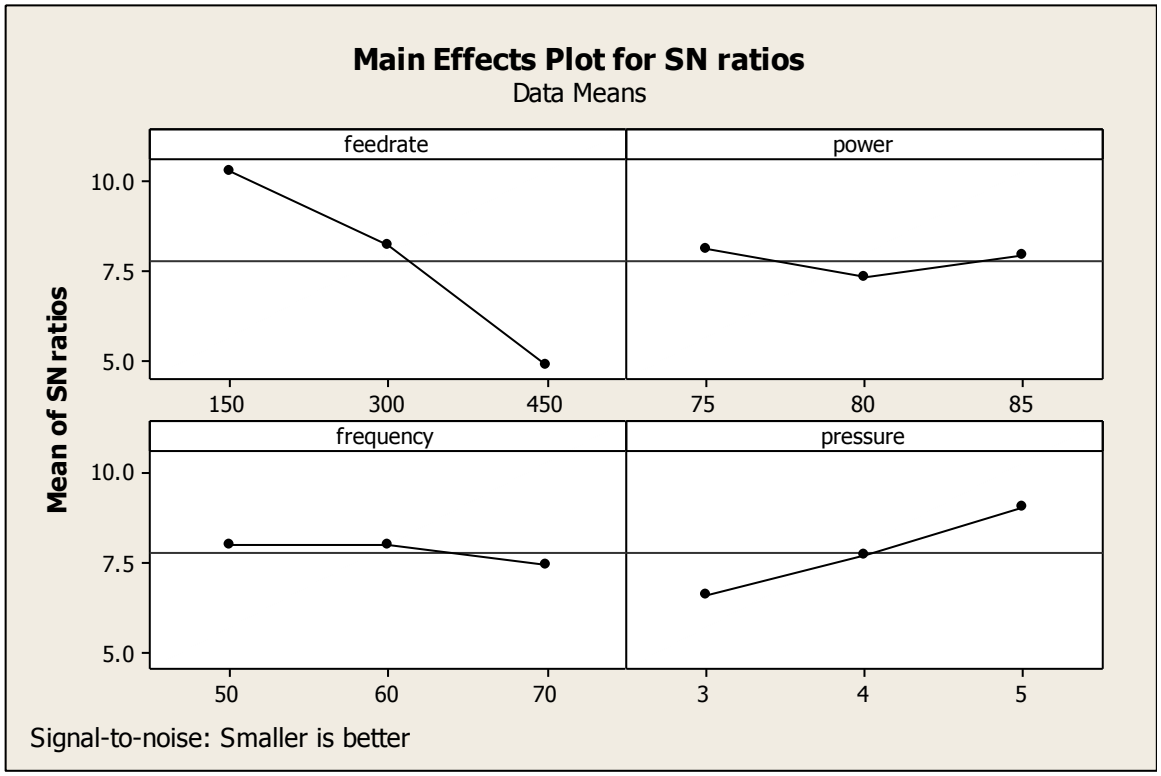

Figure 6.2 Main effects plot of K_D for S/N ratio

6.5 OPTIMAL DESIGN FOR KERF DEVIATION

In this experimental analysis, the main effect plot in Figure 6.1 used to estimate the mean kerf deviation. Kerf deviation increases when feed rate increases from 150 mm/min to 450 mm/min. and decreases when pressure decreases from 3 kg/cm^2 to 5 kg/cm^2. From the Table 6.6, it is concluded that the lowest K_D was to be observed when work piece was machined at feed rate of 150 mm/min (level 1) and gas pressure is taken at level 3 i.e. 5 kg/cm^2.

Table 6.6 Significant factors

Factor	Affecting mean		Affecting variance	
	Contribution	**Best level**	**Contribution**	**Best level**
Feed rate, A	significant	Level-1 (150mm/min.)	significant	Level-3 (450mm/min.)
Power, B	insignificant	-	insignificant	-
Gas pressure, C	significant	Level-3 (5 kg/cm^2)	insignificant	-
Frequency, D	insignificant	-	insignificant	-

Estimating the mean foe kerf deviation

In experimental analysis, the kerf deviation is a lower average response is better (LB) characteristic. Depending on the characteristic, different treatment combinations has chosen to obtain satisfactory results. After conducting the experiments the optimum treatment condition within the experiments determined on the basis of prescribed combination of factor levels was determined to one of those in the experiment.

Mean value for Kerf deviation

$$\mu_A = A_1 + C_3 - T \qquad \text{Equation...}\ldots..6.3$$

$$= 0.3009 + 0.3599 - 0.409 = 0.2518 \text{ mm}$$

Where T is given as mean K_D/no. of experiments

Confidence Interval around the Estimated Mean

The confidence interval is a maximum and minimum value between which the true average should fall at some stated percentage of confidence. The estimate of the mean μ is only a point estimate based on the averages of results obtained from the experiment. Statistically this provides a 50% chance of the true averages being greater than μ and a 50% chance of the true average being less than μ.

Confidence Interval around the estimated kerf deviation mean

$$CI_1 = \sqrt{\frac{F_{\alpha,\nu_1,\nu_2} V_e}{\eta_{eff}}} \qquad \text{Equation}\ldots\ldots..6.4$$

Where $F_{\alpha\ v1\ v2} =$ F ratio

α = risk (0.05) confidence = 1-α

v_1 = degree of freedom for mean which is always = 1

v_2 = (Total degree's of freedom) - (degree's of freedom of significant factors)

$V_e = (SS_{total}-SS_{significant\ factors})$ / (total dof – dof of significant factors)

$$\eta_{eff} = \frac{N}{1+dof_{A,c}} = \frac{9}{1+2+2} = 1.8 \qquad \text{Equation…….6.5}$$

$$CI_1 = \sqrt{\frac{F_{\alpha,v_1,v_2}V_e}{\eta_{eff}}} = \sqrt{\frac{7.71\times 0.00055}{1.8}} = 0.0484$$

So the confidence interval around the kerf deviation (K_D) is given by 0.251 ±0.048 mm.

Confirmatory Results

Experiments were conducted by taking optimal values of all factors as shown in the main effects plot of kerf deviation for means i.e. feed rate (150 mm/min), power (75W), gas pressure (5 kg/cm^2) and frequency (50Hz).

K_D =maximum top kerf width- minimum top kerf width.

Kerf deviation= 0.621-0.414 = 0.207 mm, which came out to be within range for mean kerf deviation calculated.

CHAPTER 7

CONCLUSIONS AND SCOPE OF FUTURE WORK

7.1 CONCLUSIONS

The effect of parameters i.e. feed rate, laser power, gas pressure and frequency were evaluated using ANOVA at 95 percentage of confidence level. The purpose of the ANOVA was to identify the important parameters in prediction of MRR, kerf width (K_W), and kerf deviation (K_D). Based on the experiments conducted in the present investigation, conclusions drawn from ANOVA and plots are given below:

7.1.1 MATERIAL REMOVAL RATE (MRR)

The order of ranks of four factors for material removal rate has been shown in the response table for MRR, but only feed rate is the factor which is found to be significantly affecting material removal rate with percentage contribution of 90.23. and having F value 119.217. Other factors like laser power (F value 8.126) and gas pressure (F value 3.76) has been found out to be insignificant from the output of results.

From the graph of main affects plot of MRR for means, it has been seen that with feed rate at level 3 i.e. 450 mm/min, pressure at level 1 i.e. 3 kg/cm^2 and laser power at level 1 i.e. 75 W, the optimal results can be found out with negligible affect of frequency. The confidence interval around MRR with feed rate as the significant factor has been found to be 654.8±67.88 mg/min.

For S/N response, feed rate at level 3 i.e. 450 mm/min has been found to be with highest percentage contribution of 89 percent and the only significant factor.

7.1.2 KERF WIDTH (K_W)

Feed rate (F value 19.59) has been found to be the factor significantly affecting kerf width with percentage contribution of 63.32. Kerf width first decreases with increase in power and then increases for any further increase as shown in graphs of main effects of kerf width for means though power and pressure has little effect on kerf width but these also have percentage contribution of 17.71 and 16.78 respectively.

From main effects plot for means, feed rate at level 1 i.e. 150 mm/min, power at level 2 i.e. 80W and pressure at level 3 i.e. 5 kg/cm^2 for getting minimum kerf width can be used.

In S/N ratio, feed rate (F value 49.38) and pressure (F value 21.82) has been found out to be most significant and affecting parameters for kerf width in reducing the variation.

The best results for kerf width would be suggested at feed rate of 150 mm/min i.e. at level 1 and gas pressure of 5 kg/cm^2 i.e. at level 3. The confidence interval around kerf width has been found out to be 0.512±0.165 mm.

7.1.3 KERF DEVIATION (K_D)

Feed rate (F value 526.3) and pressure (F value 90.42) with percentage contribution of 83.72 and 14.38 respectively has been found to be the factors that significantly affected the kerf deviation.

From main affects plot of kerf deviation for means, feed rate at level 1 i.e. 150mm/min and gas pressure at level 3 i.e. 5 kg/cm^2 are the factors significantly affecting output to get minimum kerf deviation.

In S/N ratio, feed rate (F value 83.61) with percentage contribution of 80.60 has been found to be the most significant factor for kerf deviation in reducing the variation. The confidence interval around the kerf deviation (K_D) is given by 0.2518 ±0.048 mm.

7.2 LIMITATIONS

The machine set up used for cutting in the present work has the maximum power capability of 100W only, which is comparatively very less than other laser machines generally used. It has the capability of cutting materials with thickness varying from range of 0.3 mm to 0.8 mm only.

The results from the experimental study are valid within the specified range of process parameters taken.

7.3 RECOMMENDATIONS FOR FUTURE WORK

A lot of research has been done in the area of laser beam cutting and great efforts have been put to improve the cutting processes. But still there are many opportunities of future work in this area. A lot of more research can be done to improve the performance.

Mild steel with ordinary grade was used as work piece material. So other materials like stainless steel with different grades can be machined or used for optimization of different parameters. As work has been done on 0.5mm thick plate, the thickness of the work piece can be varied from 0.3 to 0.8 mm sheets for this particular machine. Thickness of sheet can also be taken as the parameters for further study. Machining was carried out by taking every parameter at 3 levels. So other parameters can also be taken into account with different levels. As same assist gas (oxygen) at different levels of pressure was used to check the affect on output parameters, so by taking other types of assist gases like nitrogen, argon etc. the affect on output can be compared and parameters can be optimized.

Optimization of different laser cutting systems with different input parameters is still a vast area of research and their performances can be compared.

CHAPTER 8

REFERENCES

Black, I., Livingstone, S.A.J. and Chua, K.L. (1998), 'A laser beam machining (LBM) database for the cutting of ceramic tile', *Journal of Materials Processing Technology*, Vol. 84, pp. 47–55.

Babic, I.D., Diduck, Q., Faili, F., Wasserbauer, J., Lowe, F., Francis, D. and Ejeckam, F. (2011), 'Laser machining of GaN-on-diamond wafers', *Diamond & Related Materials*, Vol. 20, pp. 675-681.

Chang, C.W. and Kuo, C.P. (2007), 'Evaluation of surface roughness in laser-assisted machining of aluminum oxide ceramics with Taguchi method', *International Journal of Machine Tools & Manufacture*, Vol. 47, pp. 141-147.

Cicala, E., Soveja, A., Sallamand, P., Grevey, D. and Jouvard, J.M. (2008), 'The application of the random balance method in laser machining of metals', *journal of materials processing technology*, Vol. 196, pp. 393-401.

Darvishi, S., Cubaud, T. and Longtin, J.P. (2012), 'Ultrafast laser machining of tapered microchannels in glass and PDMS', *Optics and Lasers in Engineering*, Vol. 50, pp. 210-214.

Dubey, A.K. and Yadava, V. (2008), 'Experimental study of Nd:YAG laser beam machining—An overview', *journal of materials processing technology*, Vol. 195, pp. 15-26.

Dubey, A.K. and Yadava, V. (2008), 'Multi-objective optimization of Nd:YAG laser cutting of nickel-based superalloy sheet using orthogonal array with principal component analysis', *Optics and Lasers in Engineering*, Vol. 46, pp. 124-132.

Dubey, A.K. and Yadava,V. (2008), 'Multi-objective optimization of laser beam cutting process', *Optics and Laser Technology*, Vol. 40, pp. 562-570.

Ghosal, A. and Manna, A. (2012), 'Response surface method based optimization of ytterbium fiber laser parameter during machining of Al/Al2O3-MMC', *Optics & Laser Technology*, Vol. 46, pp. 67-76.

Hua, Z. and Jiawen, X. (2010), 'Modeling and Experimental Investigation of Laser Drilling with Jet Electrochemical Machining', *Chinese Journal of Aeronautics*, Vol. 23, pp. 454-460.

Hugal, H. (2000), 'New solid state lasers and their application potentials', *Optics and Lasers in Engineering*, Vol. 34, pp. 213-229.

Jiao, J. and Wang, X. (2008), 'A numerical simulation of machining glass by dual CO2-laser beams', *Optics & Laser Technology*, Vol. 40, pp. 297-301.

Karatas, C., Keles, O., Uslan, I., and Usta, Y. (2006), 'Laser cutting of steel sheets:Influence of workpiece thickness and beam waist position on kerf size and stria formation', *Journal of Materials Processing Technology*, Vol. 172, pp. 22-29.

Kasashima, N. and Kurita, T. (2012), 'Laser and electrochemical complex machining of micro-stent with on-machine three-dimensional measurement', *Optics and Lasers in Engineering*, Vol. 50, pp. 354-358.

Kang, B., Kim, G.W., Yang, M., Cho, S.H. and Park, J.K. (2012), 'A study on the effect of ultrasonic vibration in nanosecond laser machining', *Optics and Lasers in Engineering*, Vol. 50, pp. 1817-1822.

Masood, S.H., Armitage, K. and Brandt, M. (2011), 'An experimental study of laser-assisted machining of hard-to-wear white cast iron', *International Journal of Machine Tools & Manufacture*, Vol. 51, pp. 450-456.

Pandey, A.K. and Dubey, A.K. (2011), 'Intelligent Modeling of Laser Cutting of Thin Sheet', *International Journal of Modeling and Optimization*, Vol. 1, pp. 107-112.

Park, J.K., Yoon, J.W. and Cho, S.H. (2012), 'Vibration assisted femtosecond laser machining on metal', *Optics and Lasers in Engineering*, Vol. 50, pp. 833-837.

Pajak, P.T., Silva, A.K.M.D., McGeough, J.A. and Harrison, D.K. (2004), 'Modelling the aspects of precision and efficiency in laser-assisted jet electrochemical machining (LAJECM)', *Journal of Materials Processing Technology*, Vol. 149, pp. 512-518.

Powell, J., Al-Mashikhi, S.O., Kaplan, A.F.S. and Voisey, K.T. (2011), 'Fibre laser cutting of thin section mild steel: An explanation of the striation free effect', *Optics and Lasers in engineering*, Vol. 49, pp. 1069-1075.

Rajaram, N., Sheik-Ahmad, J. and Cheraghi, S.H. (2003), 'CO2 laser cut quality of 4130 steel', *International Journal of Machine Tools & Manufacture*, Vol. 43, pp. 351-358.

Romoli, L., Tantussi, G. and Dini, G. (2011), 'Experimental approach to the laser machining of PMMA substrates for the fabrication of microfluidic devices', *Optics and Lasers in Engineering*, Vol. 49, pp. 419-427.

Sobih, M., Crouse, P.L. and Li, L. (2008), 'Striation-free fibre laser laser cutting of mild steel sheets', *Materials Science and Processing*, Vol. 90, pp. 171-174.

Stelzer, S., Mahrle, A., Wetzig, A. and Beyer, E. (2013), 'Experimental investigations on fusion cutting stainless steel with fibre and Co_2 laser beams', *Physics Procedia*, Vol. 41, pp. 393-397.

Stephen, A. and Vollertsen, F. (2010), 'Mechanisms and processing limits in laser thermochemical machining', *Manufacturing Technology*, Vol. 59, pp. 251-254.

Sun, S., Brandt, M. and Dargusch, M.S. (2010), 'Thermally enhanced machining of hard-to-machine materials—A review', *International Journal of Machine Tools & Manufacture*, Vol. 50, pp. 663-680.

Tsai, C.H. and Ou, C.H. (2004), 'Machining a smooth surface of ceramic material by laser fracture machining technique', *Journal of Materials Processing Technology*, Vol. 155, pp. 1797-1804.

Yilbas, B.S. (2004), 'Laser cutting quality assessment and thermal efficiency analyses', *Journal of Materials Processing Technology*, Vol. 155-156, pp. 2106-2115.

Yang, J., Sun, S., Brandt, M. and Yan, W. (2010), 'Experimental investigation and 3D finite element prediction of the heat affected zone during laser assisted machining of Ti6Al4V alloy', *Journal of Materials Processing Technology*, Vol. 210, pp. 2215-2222.

WEB REFERENCES:

http://nptel.iitm.ac.in (downloaded on 15th Nov. 2012)

http://en.wikipedia.org/wiki/laser (downloaded on 11th Nov. 2012)

http://www.doria.fi/bitstream/handle/10024/30302/TMP.objres.256.pdf

http://books.google.co.in/books?id=HeMwJetWUG4C&printsec=frontcover&source=gbs_ge_summary_r&cad=0#v=onepage&q&f=false